HHS Public Access

Author manuscript

Nat Med. Author manuscript; available in PMC 2016 May 01.

Published in final edited form as:

Nat Med. 2015 November ; 21(11): 1307–1317. doi:10.1038/nm.3960.

PAR1 signaling regulates the retention and recruitment of EPCR-expressing bone marrow hematopoietic stem cells

Shiri Gur-Cohen[1], **Tomer Itkin**[1], **Sagarika Chakrabarty**[2], **Claudine Graf**[3], **Orit Kollet**[1], **Aya Ludin**[1], **Karin Golan**[1], **Alexander Kalinkovich**[1], **Guy Ledergor**[1,4], **Eitan Wong**[5], **Elisabeth Niemeyer**[1,6], **Ziv Porat**[7], **Ayelet Erez**[5], **Irit Sagi**[5], **Charles T Esmon**[8], **Wolfram Ruf**[2,3,*], and **Tsvee Lapidot**[1,*]

[1]Department of Immunology, Weizmann Institute of Science, Rehovot, Israel

[2]Department of Immunology and Microbial Science, The Scripps Research Institute, La Jolla, CA

[3]Center for Thrombosis and Hemostasis, Johannes Gutenberg-University Medical Center, Mainz, Germany

[6]Internal Medicine Department T, Tel-Aviv Sourasky Medical Center, Tel-Aviv, Israel

[5]Department of Biological Regulation, Weizmann Institute of Science, Rehovot, Israel

[6]Universitätsklinikum Schleswig-Holstein Campus Luebeck, Klinik für Strahlentherapie, Universitaet zu Luebeck, Germany

[7]Flow Cytometry Unit, Department of Biological Services, Weizmann Institute of Science, Rehovot, Israel

[8]Coagulation Biology Laboratory, Oklahoma Medical Research Foundation and Departments of Pathology and Biochemistry & Molecular Biology, University of Oklahoma Health Sciences Center, Oklahoma City, OK

Abstract

Retention of long-term repopulating hematopoietic stem cells (LT-HSCs) in the bone marrow is essential for hematopoiesis and for protection from myelotoxic injury. We report that signaling cascades that are traditionally viewed as coagulation-related also control retention of $EPCR^+$ LT-HSCs in the bone marrow and their recruitment to the blood via two different protease activated receptor 1 (PAR1)-mediated pathways. Thrombin-PAR1 signaling induces nitric oxide (NO) production, leading to TACE-mediated EPCR shedding, enhanced CXCL12-CXCR4-induced

Correspondence should be addressed to: Prof. Tsvee Lapidot; Tsvee.Lapidot@weizmann.ac.il, Prof. Wolfram Ruf; ruf@scripps.edu; ruf@uni-mainz.de.

AUTHOR CONTRIBUTIONS:

S.G.C. designed and performed experiments, analyzed data and wrote the manuscript; T.I. helped in the design and execution of experiments and analyzed data; S.C. performed experiments at the Scripps Research Institute, La Jolla, SD, and analyzed data; C.G. performed experiments at the Johannes Gutenberg-University Medical Center, Mainz, Germany. A.L., O.K., K.G., A.K, G.L., and E.N helped with experiments; Z.P. helped with Imaging Flow Cytometry; *ImageStream*. E.W., and I.S. helped and guided experiments related to TACE/ADAM17 prodomain inhibitor and EPCR shedding mechanism; A.E. helped in design of eNOS and nitric oxide related experiments; C.T.E. helped and guided in design EPCR and TACE/ADAM17 related experiments; W.R. designed experiments and wrote the manuscript; and T.L. designed the research and wrote the manuscript.

Competing financial interests

The authors declare no competing financial interests.

motility, and rapid stem and progenitor cell mobilization. Conversely, bone marrow blood vessels provide a microenvironment enriched with protein C that retain EPCR$^+$ LT-HSCs by limiting NO generation, reducing Cdc42 activity and enhancing VLA4 affinity and adhesion. Inhibition of NO production by activated protein C (aPC)-EPCR-PAR1 signaling reduces progenitor cell egress, increases NO^{low} bone marrow EPCR$^+$ LT-HSCs retention and protects mice from chemotherapy-induced hematological failure and death. Our study reveals new roles for PAR1 and EPCR that control NO production to balance maintenance and recruitment of bone marrow EPCR$^+$ LT-HSCs with clinical relevance.

INTRODUCTION

Most long-term repopulating hematopoietic stem cells (LT-HSCs) are retained in the bone marrow in a quiescent, non-motile mode via adhesive interactions. The homeostatic, low numbers of circulating HSCs are markedly increased as consequence to injury, bleeding and infection, a response which contributes to host defense and repair[1,2]. The chemokine CXCL12 and its major receptor CXCR4 are essential for adhesion and retention of LT-HSCs in mouse bone marrow[3]. CXCR4$^+$ LT-HSCs tightly adhere to bone marrow stromal cells, which express functional, membrane-bound CXCL12, thereby protecting LT-HSCs from myelotoxic injury[3–7]. Stress-induced secretion of CXCL12 by bone marrow stromal cells and its release into the circulation are accompanied by up-regulation of CXCR4 on hematopoietic stem and progenitor cells (HSPCs), inducing their enhanced migration[8] and recruitment to the blood[2,5,6].

Many cell types express the coagulation protease activated receptor 1 (PAR1), including bone marrow endothelial and stromal cells[9], leukocytes[10], as well as blood[11] and bone-forming progenitors[12]. The coagulation protease thrombin activates PAR1, inducing pro-inflammatory and pro-apoptotic responses[13]. Coagulation components also regulate bone structure, bone marrow HSPCs and their mobilization[14–17]. LT-HSCs in the murine fetal liver and adult bone marrow express the anticoagulant endothelial protein C receptor (EPCR) on their surface and are endowed with the highest bone marrow repopulation potential[18–21]. Binding of the protease activated protein C (aPC) to EPCR on endothelial cells results in cleavage of PAR1 at a site different from that cleaved by thrombin, enabling anti-inflammatory and cytoprotective PAR1 signaling[13,22,23] (Supplementary Fig. 1a). Treatment with aPC can rescue lethally irradiated mice[24] and promote fetal liver EPCR$^+$ HSC survival[20]. However, the roles of PAR1 signaling triggered by aPC-EPCR or thrombin in adult bone marrow LT-HSC function are not clear.

In the present study we reveal that EPCR signaling retains LT-HSCs in the bone marrow by limiting nitric oxide (NO) production and by promoting cell adhesion. In contrast, thrombin-PAR1 signaling, by inducing NO generation and EPCR shedding, mobilizes bone marrow LT-HSCs.

RESULTS

Thrombin-PAR1 signaling promotes bone marrow HSC recruitment

A minority of bone marrow HSC population endowed with the highest repopulation potential, express EPCR[18,19] with unknown functional significance. Since aPC bound to EPCR and thrombin are potent activators of endothelial PAR1 (Supplementary Fig. 1a), we first characterized PAR1 expression by HSC and found that PAR1 was highly expressed by bone marrow EPCR$^+$ LT-HSC populations (Fig. 1a,b). To test the responsiveness of HSCs to PAR1, we injected mice with thrombin, mimicking stress and injury. Active thrombin rapidly entered the bone marrow by 5 minutes after injection, followed by a decline in bone marrow thrombin activity to baseline levels by 30 minutes after injection (Fig. 1c), at which time thrombin-antithrombin (TAT) complexes had accumulated in the bone marrow (Supplementary Fig. 1b). Thrombin injection also induced a rapid, PAR1-dependent increase in the numbers of circulating leukocytes (Supplementary Fig. 1c) and immature progenitors (Fig. 1d and Supplementary Fig. 1d), which functionally expressed PAR1 (Fig. 1d). Thrombin injection led to an increase in the number of functional LT-HSCs in the blood, as assessed by a long-term competitive reconstitution assay (Fig. 1e). Notably, *F2r*$^{-/-}$ mice, deficient in PAR1, had elevated baseline levels of circulating immature LSK (Lin$^-$Sca-1$^+$c-Kit$^+$) cells; these levels were not reduced by PAR1 inhibition, confirming the specificity of PAR1 antagonism (Supplementary Fig. 1e). Upregulation of surface PAR1 levels was also detected on bone marrow LSK progenitors one hour after thrombin injection (Supplementary Fig. 1f), most likely due to enhanced recycling of PAR1 from intracellular pools[25], in agreement with data for human mobilized CD34$^+$ cells[26]. Thrombin failed to mobilize HSPCs in *F2r*$^{-/-}$ mice but not in *F2rl1*$^{-/-}$ mice deficient in PAR2 (Fig. 1f). Bone marrow chimeras revealed that both hematopoietic (donor) as well as stromal and endothelial (recipient) *F2r* were essential for thrombin-induced HSPC recruitment (Fig. 1g).

To delineate the stromal contribution for HSC recruitment induced by thrombin treatment, we confirmed PAR1 expression by bone marrow stromal cells (Fig. 1h), in line with previous work demonstrating regulation of bone marrow mesenchymal stem cell by thrombin-PAR1[27], and studied the relationship of PAR1 to CXCL12-CXCR4 signaling. Thrombin treatment decreased CXCL12 reactivity in the bone marrow (Supplementary Fig. 2a) and a PAR1-dependent increase in CXCL12 concentrations in the blood (Supplementary Fig. 2b), thereby enhancing CXCR4-dependent HSPC recruitment (Supplementary Fig. 2c – e)[6,15,28–30]. Thrombin induced PAR1-dependent CXCL12 secretion from cultured bone marrow stromal cells (Fig. 1l,m). CXCL12-induced directional migration of bone marrow progenitors was inhibited by a PAR1 antagonist (Supplementary Fig. 2f) and *F2r*$^{-/-}$ HSPCs had a reduced migration efficiency towards CXCL12 as compared to control HSPCs (Supplementary Fig. 2g). Taken together, these results demonstrate a major role for the thrombin-PAR1 pathway in modulating bone marrow CXCL12-CXCR4 chemokine signaling, leading to HSPC stress-induced recruitment to the bloodstream.

Thrombin-PAR1 signaling induces EPCR shedding and LT-HSC mobilization

Since bone marrow LT-HSCs highly express EPCR[18], we analyzed whether thrombin-induced LT-HSC mobilization resulted in the appearance of circulating EPCR$^+$ HSCs. HSC

in the bone marrow, but, unexpectedly, not in the peripheral blood, expressed EPCR; steady state or thrombin-mobilized circulating HSPCs lacked EPCR expression (Fig. 2a,b and Supplementary Fig. 3a). Thrombin-induced HSC recruitment to the bloodstream was associated with a PAR1-dependent reduction in the percentage of primitive bone marrow EPCR$^+$ LSK cells (Fig. 2c), without affecting the immature LSK pool size (Supplementary Fig. 3b). As thrombin stimulates EPCR shedding from the endothelial cell surface[31], we measured soluble EPCR (sEPCR) levels in the bone marrow after thrombin treatment. Bone marrow fluid obtained from thrombin-treated mice had increased levels of sEPCR (Fig. 2d,e). Confirming PAR1-dependent sEPCR release, thrombin failed to induce EPCR shedding in *F2r*$^{-/-}$ mice above baseline levels (Fig. 2e). Moreover, thrombin treatment of lineage-depleted bone marrow cells led to sEPCR release (Fig. 2f).

Endothelial EPCR shedding is mediated by TACE/ADAM17[32] (as illustrated in Supplementary Fig. 3c). We found that bone marrow EPCR$^+$ HSCs express TACE, in particular its non-activated precursor, as detected by an antibody to the inhibitory prodomain (Supplementary Fig. 3d). Mirroring EPCR expression, TACE prodomain was detected predominantly on primitive bone marrow HSCs, but not on circulating LSK SLAM cells (Supplementary Fig. 3e). Treatment of mice with a TACE monomeric prodomain specific inhibitor[33] prevented thrombin-induced EPCR shedding in the bone marrow (Fig. 2g) and limited stem cell mobilization (Fig. 2h). Taken together, these results demonstrate thrombin-dependent EPCR shedding from bone marrow LT-HSCs and implicate a role for TACE in stem cell recruitment.

EPCR-PAR1 signaling promotes LT-HSC retention in the BM

Our findings that EPCR shedding from bone marrow LT-HSCs is associated with stem cell recruitment suggests a functional role for EPCR in LT-HSC retention in the bone marrow. To address this possibility, we first confirmed that components of the EPCR/PAR1 system are expressed in the bone marrow. The thrombin-thrombomodulin (TM) complex converts protein C to its activated form, aPC[34] (Supplementary Fig. 1a), and previous work has shown that TM is expressed by bone marrow endothelial cells and by mature and immature hematopoietic cells[24]. We confirmed TM expression on bone marrow VE-cadherin$^+$ blood vessels (Supplementary Fig. 4a). TM-expressing blood vessels were located in close proximity to EPCR$^+$ LT-HSCs, which were unexpectedly also positive for TM staining (Fig. 3a and Supplementary Fig. 4b – c). In support of the concept that aPC is generated locally in the BM microenvironment, TM$^+$ blood vessels expressed PC/aPC (Supplementary Fig. 4d), and EPCR$^+$ stem cells were located adjacent to PC/aPC-enriched endothelial areas (Fig. 3b). Expression of TM by EPCR$^+$ LT-HSCs (Supplementary Fig. 4e) suggested that aPC generation might take place not only in the stromal compartment of the bone marrow microenvironment, but also by HSCs themselves, in line with previous work suggesting aPC generation in mature and immature hematopoietic cells[24]. Similarly to EPCR, TM was expressed by bone marrow LT-HSCs and not by circulating stem cells (Supplementary Fig. 4f).

We next studied EPCR function in LT-HSCs using adhesion assays, in which bone marrow cells were allowed to adhere to plates coated with CXCL12 and fibronectin. We found that a

large percentage of adherent, but not non-adherent, cells were primitive EPCR$^+$ LSK cells (Supplementary Fig. 5a). Adhesion of EPCR$^+$ LSK cells was reduced by a neutralizing anti-EPCR antibody that blocks aPC binding and other EPCR signaling functions[35], and adhesion was markedly enhanced by aPC stimulation (Supplementary Fig. 5b). Conversely, bone marrow LSK cells that migrate towards CXCL12 were mostly EPCR negative (Supplementary Fig. 5c).

Deletion of the gene encoding EPCR (*Procr*) in mice leads to embryonic lethality[36]. Therefore, we used viable *Procr*^{low} mice[37] with markedly reduced surface expression of EPCR on bone marrow LSK cells (Supplementary Fig. 6a). *Procr*^{low} mice had higher levels of circulating leukocytes and HSPCs in the blood (Fig. 3c and Supplementary Fig. 6b,c) and reduced numbers of primitive bone marrow HSCs (Fig. 3d), compared to wild-type control mice. Consistent with a defect in HSPC retention, *Procr*^{low} bone marrow LSK progenitor cells had an increased migration capacity towards CXCL12 and decreased adhesion to immobilized CXCL12/fibronectin (Supplementary Fig. 6d,e). Reduced bone marrow HSC retention in *Procr*^{low} mice was associated with an increased frequency of HSCs in the spleen (Supplementary Fig. 6f). Similarly to *Procr*^{low} mice, *F2r*$^{-/-}$ mice exhibited increased numbers of HSPCs in the circulation (Fig. 3e) and reduced bone marrow HSC retention (Fig. 3f), with no significant changes in the number of HSCs in the spleen (Supplementary Fig. 6g).

Thbd$^{Pro/Pro}$ mice carry a mutation in the gene encoding TM that impairs thrombin binding to TM, limiting aPC generation and thereby causing chronically deregulated control of thrombin generation[38]. *Thbd*$^{Pro/Pro}$ mice also demonstrated higher levels of HSPCs in the circulation (Supplementary Fig. 6h), whereas aPC treatment of these mice partially reversed this phenotype (Supplementary Fig. 6h). Consistent with the concept that increased HSPC egress in *Thbd*$^{Pro/Pro}$ mice is due to a reduction in aPC generation, TM expression on bone marrow LT-HSCs was similar between wild-type and *Thbd*$^{Pro/Pro}$ mice, and EPCR expression on bone marrow HSCs was even slightly elevated in *Thbd*$^{Pro/Pro}$ as compared to wild-type mice (Supplementary Fig. 6i,j).

To functionally test the role of EPCR in LT-HSC BM retention, we performed long-term competitive hematopoietic reconstitution experiments with bone marrow from *Procr*^{low} mice. Compared to control wild-type HSCs, bone marrow HSCs obtained from *Procr*^{low} mice showed markedly reduced competition with wild-type bone marrow cells (Fig. 3g). Furthermore, functional antagonism of EPCR reduced HSC competitive long-term bone marrow repopulation ability (Fig. 3h). Taken together, these results indicate that a functional aPC-EPCR-PAR1 signaling pathway is present in the bone marrow microenvironment that regulates EPCR$^+$ LT-HSCs BM retention and long-term repopulation potential.

aPC-EPCR-PAR1 signaling regulates HSC adhesion

In LT-HSCs, regulation of Cdc42 activity and its polar distribution is crucial for cell adhesion and bone marrow repopulation potential[39,40]. We found a random distribution of Cdc42 in immature bone marrow EPCR negative LSK cells, whereas primitive EPCR$^+$ LSK cells showed a polar Cdc42 distribution (Fig. 4a). Blockade of ligand binding to EPCR induced Cdc42 depolarization (Fig. 4b), and bone marrow PAR1 deficient *F2r*$^{-/-}$ EPCR$^+$

SK SLAM cells also lacked polar Cdc42 distribution (Supplementary Fig. 7a). Cdc42 polarity correlates with low Cdc42 activity in HSC[41]. Bone marrow EPCR$^+$ HSCs expressed lower levels of active Cdc42 (Cdc42–GTP) compared to EPCR$^-$ SK SLAM cells (Fig. 4c and Supplementary Fig. 7b). Moreover, EPCR blockade abrogated Cdc42 polarity (Fig. 4b) and increased Cdc42–GTP levels (Fig. 4d and Supplementary Fig. 7c). Accordingly, LSK SLAM bone marrow cells from *Procr^{low}* mice, as compared to those from wild-type mice, showed elevated Cdc42 activity and reduced adhesion; the effect on adhesion was reversed by *in vitro* treatment with the Cdc42 inhibitor, CASIN (Supplementary Fig. 7d,e). These data indicate that EPCR signaling controls Cdc42 polarity and activity in HSCs and thereby cell adhesion.

We found that the adhesion molecule integrin α4β1 (VLA4), which binds fibronectin and VCAM-1 and is crucial for bone marrow HSC retention[1,42], was expressed at higher levels by bone marrow EPCR$^+$ LSK as compared with EPCR$^-$ LSK cells (Fig. 4e and Supplementary Fig. 8a) or circulating primitive progenitors (Supplementary Fig. 8b). Accordingly, integrin α4β1 on bone marrow EPCR$^+$ HSCs had higher affinity for ligand binding as compared to integrin α4β1 on bone marrow EPCR$^-$ HSCs (Supplementary Fig. 8c). Importantly, aPC treatment increased integrin α4β1 affinity in wild-type but not *Procr^{low}* bone marrow LT-HSCs in an EPCR-dependent manner (Fig. 4g), despite similar VLA4 expression (Fig. 4h). In addition, *F2r$^{-/-}$* bone marrow stem cells had normal VLA4 expression, but their integrin α4β1 affinity was lower compared to wild-type stem cells (Fig. 4i). Cdc42 inhibition by CASIN increased the α4β1 affinity of bone marrow HSCs (Supplementary Fig. 8d), linking Cdc42 function to affinity modulation of α4β1 integrin. The effect of CASIN on α4β1 affinity was specific, since a conformational antibody to β1 integrins, which are generally crucial for HSC function and bone marrow retention[43,44], bound similarly to CASIN-treated and untreated wild-type bone marrow HSCs, and also bound similarly to wild-type, *Procr^{low}* and *F2r$^{-/-}$* bone marrow HSCs (Supplementary Fig. 8e – g).

A neutralizing anti-VLA4 antibody mobilizes LT-HSCs to the blood[42], indicating that VLA4 is crucial for HSC retention in the bone marrow . We found that low surface CXCR4 expression on bone marrow EPCR$^+$ HSCs was rapidly upregulated by EPCR neutralization (Supplementary Fig. 8h), and repeated *in vivo* EPCR neutralization mobilized HSCs to the blood, similarly to VLA4 blockade (Fig. 4j). Interestingly, blockade of EPCR or VLA4 led to mobilization of LT-HSCs that retained EPCR expression in the blood circulation (Fig. 4j). Taken together, these data show that aPC-EPCR-PAR1 signaling leads to a low level of Cdc42 activity, increased VLA4 affinity and retention of EPCR$^+$ LT-HSCs in the bone marrow.

Nitric oxide production overcomes HSC retention in the bone marrow

We next sought to understand the mechanism by which thrombin-PAR1 signaling induces EPCR shedding to counteract EPCR-dependent adhesion. NO signaling is essential for the initiation of hematopoiesis during embryonic development[45,46], and endothelial nitric oxide synthase (eNOS, encoded by *Nos3*) activity by bone marrow stromal cells is essential for the mobilization of endothelial progenitor cells[47]. NO production is activated by eNOS

phosphorylation at Ser1177 and negatively regulated by eNOS phosphorylation at Thr495[48]. We found that circulating SLAM cells contain higher intracellular NO levels compared with bone marrow-retained stem cells (Fig. 5a). Notably, thrombin injection rapidly increased NO levels in bone marrow HSCs (Supplementary Fig. 9a) and eNOS phosphorylation at Ser1177 in immature LSK cells (Fig. 5b,c). Specificity of the NO probe was demonstrated by pretreatment of HSCs with the NOS inhibitor L-NAME (*N*-nitro-L-arginine methyl ester) (Supplementary Fig. 9b). Pharmacological inhibition of NO generation by L-NAME markedly reduced thrombin-induced HSPC recruitment and prevented EPCR shedding by bone marrow LT-HSCs (Fig. 5d).

Next, we generated chimeric mice with *Nos3* deficiency in either hematopoietic (donor) or stromal cells (recipient). In support of the concept that eNOS has an intrinsic role in HSCs, thrombin injection in chimeric mice with hematopoietic deficiency of *Nos3* failed to increase circulating LSK levels and to diminish the percentage of bone marrow $EPCR^+$ LSK cells (Fig. 5e). Thrombin also failed to mobilize LSK cells in $Nos3^{-/-}$ mice (Supplementary Fig. 9c). Pharmacological elevation of NO levels in $Nos3^{-/-}$ mice with the NO donor SNAP induced LSK cell mobilization and decreased the percentage of bone marrow $EPCR^+$ LSK cells (Supplementary Fig. 9d,e). Accordingly, injection of SNAP into wild-type mice rapidly mobilized immature LSK cells and reduced the numbers of EPCR-expressing bone marrow LSK cells (Fig. 5f). TACE inhibition abrogated the effects of SNAP on stem cell mobilization and reduction of $EPCR^+$ by HSC in the bone marrow (Supplementary Fig. 9f,g). Moreover, the rapid, thrombin-induced disappearance of TACE prodomain expression by primitive bone marrow HSCs was blocked by L-NAME pretreatment (Supplementary Fig. 9h), suggestive of NO-dependent TACE activation. Thrombin injection rapidly induced loss of the polar pattern of Cdc42 distribution in bone marrow $EPCR^+$ HSCs and reduced EPCR staining intensity (Fig. 5g), indicative of EPCR shedding. NOS inhibition with L-NAME prevented the thrombin-induced increase in Cdc42-GTP content (Fig. 5h), whereas treatment with the NO donor SNAP elevated Cdc42-GTP activity and reduced VLA4 affinity on bone marrow LT-HSCs (Fig. 5i). These results position thrombin-PAR1 signaling upstream of NO production, which in turn promotes Cdc42 activity and TACE-mediated EPCR shedding from bone marrow stem cells.

aPC-EPCR-PAR1 signaling restricts NO production in bone marrow LT-HSCs

Since thrombin/PAR1 signaling overcomes EPCR-mediated bone marrow LT-HSC retention by elevating NO levels, we further measured NO content in bone marrow LT-HSCs. Bone marrow $EPCR^+$ LSK cells had lower intracellular NO levels compared to EPCR negative LSK cells (Fig. 6a). Interestingly, NO content was elevated in bone marrow stem cells from $Thbd^{Pro/Pro}$ mice (Supplementary Fig. 10a), which have impaired aPC generation, as well as in bone marrow stem cells from *F2r*-deficient mice (Supplementary Fig. 10b). Blockade of EPCR function increased intracellular NO content in primitive HSCs (Fig. 6b). Moreover, $Procr^{low}$ bone marrow LT-HSCs had higher baseline intracellular NO levels than wild-type LT-HSCs, and treatment with aPC reduced NO content in wild-type but not $Procr^{low}$ bone marrow LT-HSCs (Fig. 6c). Most $EPCR^-$ and $EPCR^+$ SLAM HSCs in the bone marrow showed low levels of activating eNOS Ser1177 phosphorylation; however, the majority of $EPCR^+$ SLAM HSCs, but only a minority of $EPCR^-$ SLAM HSCs,

stained positive for inhibitory eNOS Thr495 phosphorylation (Supplementary Fig. 10c,d). aPC treatment of SK SLAM HSCs increased eNOS phosphorylation at Thr495, while causing gradual dephosphorylation at Ser1177 (Fig. 6d), in a PAR1-dependent manner (Supplementary Fig. 10e – f). Moreover, neither chloromethylketone-inactivated aPC nor the alternative EPCR ligand factor VIIa induced eNOS Thr495 phosphorylation in bone marrow SLAM LSK cells (Fig. 6e). Thus, proteolytic aPC-EPCR-PAR1 signaling imposes inhibitory eNOS phosphorylation and thereby limits NO generation in bone marrow EPCR$^+$ LSK cells.

Next, to suppress NO generation in the absence of EPCR signaling, we treated chimeric mice reconstituted with *Procr*^{low} bone marrow with L-NAME. This intervention reduced the elevated levels of circulating LSK cells (Fig. 6f). *In vitro*, L-NAME treatment normalized the behavior of *Procr*^{low} LSK cells in adhesion and migration assays (Fig. 6g). Since EPCR$^+$ HSCs possess the highest long-term repopulation potential[18,19], we tested whether limiting NO levels *in vivo* can increase LT-HSC repopulation potential. Prolonged L-NAME treatment preferentially reduced immature LSK cell egress to the blood and induced preferential expansion of primitive bone marrow EPCR$^+$ LSK cells (Fig. 6h) and quiescent CD34$^-$ LSK cells (Supplementary Fig. 11a). Egress of maturing leukocytes (Supplementary Fig. 11b), bone marrow cellularity and total immature LSK progenitor cell levels (Supplementary Fig. 11c,d) were minimally affected. Competitive, long-term bone marrow reconstitution assays revealed increased multi-lineage repopulation following L-NAME pre-treatment of donor mice (Fig. 6i and Supplementary Fig. 11e), with balanced myeloid/lymphoid reconstitution (Supplementary Fig. 11f) and higher levels of donor type EPCR$^+$ LT-HSCs (Supplementary Fig. 11g). Of note, transplantation using half the cell dose of donor bone marrow cells from L-NAME pre-treated mice still gave rise to higher reconstitution levels compared to the full cell dose of bone marrow cells from PBS pre-treated mice (Fig. 6i). Similarly, treatment of mice with aPC reduced mature and immature leukocyte egress (Supplementary Fig. 12a,b), preferentially expanded quiescent CD34$^-$ LSK and primitive bone marrow EPCR$^+$ LSK cell populations (Supplementary Fig. 12c – f) and increased competitive bone marrow reconstitution (Supplementary Fig. 12g).

Retention of HSCs in supportive stromal niches in the bone marrow is essential to maintain HSC quiescence and to protect HSCs from myeloablation[3]. We therefore evaluated the role of EPCR-PAR1 signaling in protecting mice from mortality induced by 5-FU chemotherapy. Treatment with the NO donor SNAP sensitized mice to 5-FU-induced death (Fig. 6j), indicating that suppression of NO production has a crucial role in survival after myeloablation. *F2r*$^{-/-}$ mice, as well as mice treated with a neutralizing anti-EPCR antibody, were also susceptible to mortality induced by 5-FU treatment, as compared to control mice (Fig. 6j). These results suggest that aPC-EPCR-PAR1 signaling, by limiting NO production, retains EPCR$^+$ LT-HSCs in the bone marrow and protects them from chemotherapy insult.

DISCUSSION

In the current study, we discovered a new role for factors traditionally viewed as functioning in coagulation and inflammation pathways in regulating LT-HSC function within the bone marrow microenvironment. Our results reveal that, beyond its role in hemostasis, PAR1 acts

through distinct signaling cascades to promote or inhibit NO production by LT-HSCs. PAR1 retains bone marrow EPCR-expressing HSC through suppression of NO production and mediates stem cell recruitment through elevation of NO levels, EPCR shedding and activation of Cdc42 (Supplementary Fig. 13a,b).

EPCR was recently identified as a stem cell marker in various organs[11], including murine fetal liver and adult bone marrow LT-HSCs[18–21] and mammary stem cells[49], and its function is crucial for breast cancer stem cell phenotypes and tumor progression[50]. We found that EPCR ligand-dependent signaling occurs within a TM and PC-enriched endothelial microenvironment in the bone marrow. Consistent with our findings, mice harboring a *Procr* mutation that disables all ligand binding to EPCR, including binding by PC/aPC, exhibit bone marrow failure and splenomegaly[51]. We further show that EPCR-PAR1 signaling functionally regulates anchorage and bone marrow retention of LT-HSCs by restricting NO production and Cdc42 activity, leading to increased α4β1 affinity (Supplementary Fig. 13a). While the ultimate consequence of the endothelial-to-hematopoietic transition during ontogeny is downregulation of the endothelial program in blood-forming stem cells and mature leukocytes, bone marrow-retained LT-HSCs preserve expression of some endothelial genes, such as those encoding EPCR[18–21] and vWF[52]. Our findings indicate that LT-HSCs in the adult bone marrow preserve endothelial expression of TM and EPCR that ultimately maintain stem cells with low NO levels and protect from DNA damaging agents and cell death[20,24].

Based on these and previous findings[24], we propose that the homeostatic bone marrow stem cell niche represents a TM-enriched microenvironment that can initiate local aPC generation, which functionally retains long-term repopulating $EPCR^+$ stem cells. Similarly to endothelial cells, bone marrow $EPCR^+$ LT-HSCs express surface TM, implying the possibility of autocrine aPC generation. Recently, megakaryocytes were found to negatively regulate bone marrow HSC proliferation via secretion of platelet factor 4 (PF4)[53,54]. PF4 also supports TM-dependent aPC generation[55], suggesting that megakaryocytes may participate in the TM^+ niche for $EPCR^+$ stem cells, enhancing aPC generation and thereby contributing to LT-HSC bone marrow retention and protection. Indeed, under chemotherapeutic stress conditions, PF4 secretion by megakaryocytes promotes HSC expansion[53], in agreement with our results that aPC-EPCR signaling restricts NO production, expands bone marrow LT-HSCs and protects them from chemotherapy insult.

Recently we discovered a rare population of radiation resistant αSMA^+ $COX2^+$ macrophages, which maintain bone marrow LT-HSCs and protect them from inflammatory insult by limiting ROS production via PGE2 secretion[56]. In the current study, we reveal that limiting NO production via aPC-EPCR-PAR1 signaling induces LT-HSC retention in the bone marrow and protection from chemotherapy-induced mortality. PAR1 signaling in bone marrow LT-HSCs regulate NO generation through balanced control of eNOS phosphorylation at two regulatory sites (Supplementary Fig. 13c). aPC-EPCR-PAR1 signaling leads to increased eNOS phosphorylation at the negative regulatory site Thr495, and reduced phosphorylation at the positive regulatory site Ser1177, maintaining bone marrow LT-HSCs with low NO levels. Low NO in turn limits Cdc42 activity, which is required for LT-HSC adhesion and bone marrow retention. Similarly to breast cancer stem

cells where EPCR regulates proliferation on matrices that engage VLA4[50], aPC-EPCR-PAR1 signaling in bone marrow LT-HSCs increases VLA4 affinity. Our results are consistent with previous findings implicating elevated Cdc42 activity in the reduced function of aged HSCs, in which Cdc42 polarity is attenuated[40,41], associated with loss of cell adhesion and function[57,58].

LT-HSCs must exit quiescence and overcome bone marrow retention in order to ensure homeostatic as well as stress-induced blood cell production. Our findings reveal that thrombin and NO generation are required to address the changing demands for new blood cell production. Physiological stress, inflammation and cytokine-induced mobilization transiently increase thrombin generation[59]. Our model suggests that increased thrombin levels directly activate PAR1 signaling cascades in bone marrow LT-HSCs as well as in stromal cells (Supplementary Fig. 13b), inducing stem cell egress and recruitment to the blood circulation as part of host defense and repair. A shift in eNOS phosphorylation at the activating Ser1177 site through thrombin-PAR1 signaling initiates NO production that enable bone marrow LT-HSC migration and recruitment. Consistent with our findings, signaling driven by NO production potentiates stem cell migration, leading to hematopoiesis during mouse fetal development[45,46,60]. Conversely, we found that reducing NO levels preferentially retains the undifferentiated LT-HSC pool in the bone marrow via adhesive interactions with stromal cells.

We found that thrombin-dependent shedding of EPCR by TACE/ADAM17[32] overcomes LT-HSC retention in the bone marrow, such that circulating stem cells in the blood lack EPCR expression (Supplementary Fig. 14). Since low levels of thrombin can initiate aPC production[34], it is conceivable that homeostatic, low levels of thrombin regulate LT-HSC retention in the bone marrow by generating aPC, whereas stress-induced, transiently increased thrombin levels induce LT-HSC recruitment Bone marrow-retained LT-HSCs and stem cells in the circulation can be functionally distinguished by differences in intracellular NO content (Supplementary Fig. 14). Thrombin-mobilized stem cells maintain their long-term repopulation potential and re-express EPCR in the bone marrow after transplantation. However, future studies at the single cell level will reveal whether these cells can revert back from a state with high NO levels to a bone marrow-retained stem cell with low intracellular NO content. While our results mainly focus on the major role of eNOS in the maintenance of bone marrow LT-HSCs, it should be noted that other NOSs, namely iNOS and nNOS, which are expressed at low levels by LT-HSCs, might also be involved and regulated by PAR1 signaling. Previous work demonstrated that iNOS knockdown did not affect the *runx1/cmyb* gene complex that regulates HSC differentiation to mature blood cells[45]. In our study, eNOS-deficient mice failed to mobilize stem cells in response to thrombin stimulation.

Our results reveal that PAR1 signaling, under the direction of two different proteases, thrombin and aPC, acts to switch stem cell function. This switch dictates stem cell localization and activation states, regulating stem cell retention in the bone marrow, susceptibility to chemotherapy insult, migration and repopulation potential. Harnessing of this switch has the potential to improve clinical stem cell mobilization and transplantation protocols as well as the resistance of stem cells to chemotherapy.

ONLINE MATERIALS AND METHODS

Animals

C57BL/6 (CD45.2) and BALB/c mice were purchased from Harlan Laboratories (Rehovot, Israel). B6.SJL (CD45.1) mice were bred at the Weizmann Institute of Science. *Nos3*$^{-/-}$ mice were purchased from Jackson Laboratories. Transgenic *Procr*^{low} mice that express <10% EPCR were generated as described[37]. *F2r*$^{-/-}$ and *F2rl1*$^{-/-}$ mice provided by Dr. P. Andrade-Gordon[61,62] were backcrossed to C57BL/6 mice. *Thbd*$^{Pro/Pro}$ mice provided by Dr. H. Weiler, carrying a TM gene mutation that disrupts thrombin binding and TM-dependent activation of protein C, have been previously described[38]. Breeding and all experimental procedures were monitored by the Veterinary Resources Unit of the Weizmann Institute and were approved by the Institutional Animal Care and Use Committee (IACUC). Experiments with *Procr*^{low}, *Thbd*$^{Pro/Pro}$, *F2r*$^{-/-}$ and *F2rl1*$^{-/-}$ mice were performed at the Scripps Research Institute, La Jolla, CA, USA or at the Johannes Gutenberg-University Medical Center, Mainz, Germany under approved protocols of the Scripps Research Institute (TSRI) IACUC or under protocols issued by the state of Rhineland-Palatinate. All transgenic mice with homozygous mutations were compared to strain matched wild-type C57BL/6 sex- and age-matched controls. BALB/c mice were used for anti-CXCR4 injections. 8–12-week-old mice, both male and female, were used for all experiments. Bone marrow cells were obtained by flushing long bones with phosphate-buffered saline, and peripheral blood was collected from the heart using heparinized syringes.

In vivo and *in vitro* treatments

Thrombin was purchased from Sigma (T7513, specific activity of 2,000 NIH units/mg) or Haematologic Technologies (BCT-1020, specific activity of 3,800 NIH units/mg) and was injected intraperitoneally at 250 U/kg or was used *in vitro* at 1 U/ml concentration. The PAR1 antagonist SCH79797 (TOCRIS, cat#1592), was injected intraperitoneally at 0.5 mg/kg 1 hour before thrombin administration. For *in vitro* stimulation SCH79797 was used at 200 nM, 30 minutes before thrombin stimulation. L-NAME (*N*-nitro-L-arginine methyl ester, Sigma N5751) was used either for short-term treatment, injected once intraperitoneally at 30 mg/kg either alone or in the case of thrombin treatment experiments 30 minutes before and again at the time of thrombin injection or for long-term treatment, injected once a day intraperitoneally for 5 days. For *in vitro* stimulation, bone marrow mononuclear cells (MNC) were pretreated for 2 hours with 5 mM L-NAME prior to seeding on fibronectin/CXCL12-coated plates (25 μg/ml fibronectin and 2.5 μg/ml CXCL12, as detailed in the adhesion assay). SNAP (*S*-Nitroso-*N*-acetyl-DL-penicillamine, Sigma N3398) was injected intraperitoneally at 5 mg/kg and mice were sacrificed 60 minutes later. For *in vitro* stimulation, SNAP was used at 10 μM for different time points as indicated. CASIN (Xcessbio Bioscience, M60040-2s) was used *in vitro* at 5 μM at different time points. TACE monomeric prodomain inhibitor was developed and produced as previously described[33]. The TACE inhibitor was used *in vitro* at 1 μM and *in vivo* at 25 μg/mouse and was administrated intravenously 1 hour before SNAP or thrombin treatment. For neutralization of CXCR4, we used a total of 50 μg mouse anti-human CXCR4 antibody (clone 12G5, R&D Systems), which is cross-reactive to murine CXCR4[28], is nontoxic and neutralizes CXCR4 *in vivo*[6]. Anti-CXCR4 antibody or IgG isotype control (BD Pharmingen, 556651) were first injected

into the peritoneum (25 μg in PBS) followed by intravenous injection of an additional 25 μg dose of antibody 30 minutes later, with or without thrombin treatment intraperitoneally, and mice were sacrificed 60 minutes after thrombin stimulation. Neutralizing (clone 1560) and non-neutralizing rat anti-mouse antibodies (clone 1562) to EPCR were produced in the laboratory of Dr. C.T. Esmon and were used as previously described[35]. The EPCR neutralizing antibody blocks EPCR signaling transmitted via PARs and driven by aPC or other proteases that interact with EPCR. Bone marrow MNCs were treated *in vitro* with 10 μg/ml of anti-EPCR antibody at 37 °C for 30 minutes prior to loading onto transwells or fibronectin/CXCL12-coated plates, or for 60 minutes for Cdc42 polarity and VLA4 affinity assays. For *in vivo* treatments, EPCR neutralizing and non-neutralizing antibodies were injected intraperitoneally at 50 μg/mouse for 3 days and mice were sacrificed 2 hours after the last injection for mobilization studies. Similarly, anti-VLA4 antibody (Southern Biotech, 1620-01 clone PS/2) was injected *in vivo* at 50 μg/mouse for 3 days and mice were sacrificed 2 hours after the last injection. Mouse aPC was produced by CT Esmon[63] and used to stimulate cells *in vitro* at 1 μg/ml for 1 hour, and *in vivo* at 10 μg/mouse once a day for 5 days in wild-type mice for HSC expansion studies, or twice a day for 3 days in $Thbd^{Pro/Pro}$ mice. Human aPC was purchased from Sigma (P2200, ≥90% purity) and used to stimulate cells *in vitro* at at 1 μg/ml for 1 hour. FVIIa or active-site blocked FVIIa were obtained from Novo Nordisk (Måløv, Denmark) and were used *in vitro* at 1 μg/ml for 15 minutes. All *in vitro* treatments were carried out at 37 °C in a 5% CO_2 humidified incubator.

5-FU treatment *in vivo*

Mice were administrated intraperitoneally with non-neutralizing (clone 1562) or neutralizing (clone 1560) rat anti-mouse ECPR antibody (50 μg/mouse) or with SNAP (5 mg/kg) for 3 days. On the 3rd day, SNAP was co-administrated with 5-FU (EBEWE Pharma, 150 mg/kg intraperitoneally). This treatment regimen was repeated once weekly. Mouse survival was monitored for 30 days and analyzed with Prism 4.0c.

Flow cytometry

Cell populations were analyzed with a FACSCalibur instrument (Becton-Dickinson) with CellQuest software, with a MacsQuant instrument (Miltenyi, Bergisch Gladbach, Germany) or with a FACS LSRII instrument (BD Biosciences) with FACSDiva software. Data were analyzed with FlowJo (Tree Star) or MacsQuant. Flushed bone marrow cells were stained for 30 minutes at 4°C in flow cytometry buffer (PBS, 10% FCS and 0.02% azide). For antigens that require intracellular staining (p-eNOS and Cdc42), cell surface staining was followed by cell fixation and permeabilization with the Cytofix/Cytoperm kit (BD Biosciences) according to the manufacturer's instructions. For LSK staining, we used a lineage cocktail of either FITC-conjugated antibodies to CD4 (GK1.5), CD8 (53–6.7), B220 (RA3-6B2), CD11b (M1/70), Gr-1 (RB6-8C5) and Ter119 (TER-119) (all from Biolegend) or a biotinylated lineage cocktail (Miltenyi), together with anti Sca-1-PE (D7) or Sca-1-PE-Cy7 (D7) and anti c-Kit-APC (2B8) (all from Biolegend). For SLAM staining, we used biotinylated anti-CD150 or anti-CD150 PerCP-Cy5.5 (TC15-12F12.2, Biolegend) together with anti CD48-PE (HM48-1, BD Bioscience) or CD48-Pacific Blue (HM48-1, Biolegend). CD34 expression on LSK cells was analyzed using anti CD34-eFlour 450 (RAM34, eBiosciences). After staining for cell surface antigens, intracellular NO was detected by

incubation of cells for 15 minutes at 37 °C with 10 μM DAF-FM diacetate followed by extensive washing, according to the manufacturer's instructions (Molecular Probes). Staining without addition of the DAF-FM probe was considered to be the baseline for gating the positive population. CXCR4 was stained with rabbit anti-rat CXCR4 (Torrey Pines Biolabs, TP503)). Stromal precursors were identified using CD31-Pe-Cy7 (390), CD45-FITC (30-F11), Sca-1-PE (D7) and PDFGRα-APC (APA5) (all from Biolegend). PAR1 was detected by using rabbit anti mouse PAR1 (H111, Santa Cruz). EPCR was detected by using either biotinylated anti-CD201 or conjugated anti-EPCR-PE, EPCR-APC or EPCR-PerCP-eFluor 710 (clone 1560, all from eBioscience). TACE was identified using rabbit anti-mouse TACE (Santa Cruz, H-170). TACE prodomain was detected by using rabbit anti-mouse TACE prodomain antibody, provided by C. Blobel. eNOS phosphorylation was detected using anti-p-eNOS Ser1177 (C9C3) or Thr495 (T495), both from Cell Signaling. Cdc42 was detected using rabbit anti-mouse Cdc42 (Millipore, 07–1466). For bone marrow endothelial cell staining, bone marrow cells were flushed with and mechanically crushed mortar and pestle in LDM medium (Invitrogen) supplemented with 0.1% DNase 1 (Roche), followed by 30 minutes digestion at 37 °C with shaking. Following incubation, cells were washed and underwent red blood cell lysis (Sigma, R7577) before staining with rat anti-mouse TM (clone 461714, R&D) followed by anti-rat 488 (Jackson ImmunoResearch) or TM-FITC conjugated antibody (clone 461714, R&D) and Sca-1-PE, CD45-APC, CD31-Pe-Cy7 (all from Biolegend). All antibody catalog numbers, clones and manufacturers can also be found in the Supplementary Table 1.

VLA4 affinity assay

For integrin α4β1 (VLA4) detection, we used rat anti mouse-VLA4 (PS/2, Southern Biotech) or conjugated rat anti-mouse VLA4 FITC (R1–2, eBioscience). For the VLA4 affinity assay, bone marrow cells were flushed with HBSS medium (Gibco) supplemented with 1 mM $CaCl_2$, 1 mM $MgCl_2$ and 20 mM HEPES (LDV medium). Five million cells were either non-stimulated or stimulated as indicated in a total volume of 100 μl in the presence of 10 nM LDV-FITC (fluorescent ligand that binds to the $\alpha_4\beta_1$ integrin with high affinity, R&D catalog number 4577) in LDV medium. Following incubation, cells were put on ice, fixed with 4% paraformaldehyde for 10 minutes and stained for 30 minutes with Sca-1/c-Kit/SLAM/EPCR in the presence of $PBS^{+/+}$ (PBS supplemented with calcium chloride and magnesium chloride). Cells were resuspended in 300 μl $PBS^{+/+}$ for analysis by flow cytometry with negative control samples stained with LDV-FITC in the presence of EDTA.

Colony-forming assays (CFU-C)

Peripheral blood MNCs were isolated by Ficoll (Lymphoprep) separation and were seeded (2×10^5 cells/mL) in semisolid cultures supplemented with EPO (2 U/ml, obtained from Orto BioTech, Don Mills, Canada), IL-3, GM-CSF (both obtained from Kirin Brewery Company, Tokyo, Japan) and SCF (PeproTech) as previously described[28]. Colonies, reflecting colony-forming unit cells (CFU-C), were scored 7 days after plating and presented as CFU-C/ml of blood.

Migration assay

Bone marrow MNCs were isolated by Ficoll separation and migration assays were performed in transwell chambers (Costar) as previously described[28]. Briefly, 2 x 10^5 bone marrow MNCs were added to the upper transwell for migration towards 125 ng/ml CXCL12 (PeproTech, Rocky Hill, NJ, USA) for 2 hours in full RPMI 1640 medium (Gibco) containing 10% FCS. Following migration, cells from the upper well (referred to as non-migrating cells) and cells from the bottom chamber (referred to as migrating cells) were stained for LSK or LSK/EPCR and analyzed by flow cytometry.

Adhesion assay

Non-tissue culture 6-well plates (Corning) were coated with 25 μg/ml fibronectin (Sigma) and 2.5 μg/ml CXCL12 (PeproTech, Rocky Hill, NJ, USA) overnight at 4 °C. The plates were subsequently washed with PBS and blocked with 2% BSA for 30 minutes at room temperature. Bone marrow MNCs (5 x 10^6) cells were seeded in RPMI 1640 medium (Gibco) containing 10% FCS and then allowed to adhere to the coated plates for 2 hours at 37 °C. Non-adherent cells were collected by gently rinsing with the medium. To collect adherent cells, plates were gently washed three times with PBS followed by incubation with cell dissociation buffer (Gibco, Carlsbad, CA) and vigorously rinsing the plates with PBS. The cells were then stained for LSK or EPCR/LSK expression and analyzed by flow cytometry.

CXCL12 ELISA

Levels of functional CXCL12 in plasma and bone marrow were determined as described[28]. Total protein content in bone marrow fluid was quantified by Bradford assay and CXCL12 concentration in bone marrow fluid was normalized to protein content.

sEPCR ELISA

Mouse sEPCR ELISA (Biotechnology Systems, M7888) was used to determine sEPCR content following thrombin stimulation *in vitro*. In some experiments, total bone marrow cells were lineage depleted using mouse lineage depletion kit (BD) according to the manufacturer's instructions. The lineage depleted cell fraction (5 x 10^6 cells) was stimulated with either PBS or thrombin (1 U/ml) for 45 minutes at 37 °C. Following incubation, supernatants were collected to measure sEPCR. To determine sEPCR content following thrombin treatment *in vivo*, wild-type and *F2r*$^{-/-}$ mice were treated with thrombin and sacrificed 1 hour later. Bones were flushed in 300 μl PBS and supernatants were collected to measure sEPCR based on an sEPCR standard curve and normalization to total protein in the sample, as determined using the Bradford reagent.

aPC and FVIIa inactivation

Mouse activated protein C was active site blocked by incubation with 100 μM 1,5-DNS-GGACK (EMD 251700, Calbiochem) for 3 days at 4 °C, followed by extensive dialysis against HBS (Hepes buffered saline). The protein concentration was determined and loss of catalytic activity towards a chromogenic substrate (Spectozyme aPC) was verified. FVIIa inactivation was performed as previously described[64].

Chromogenic thrombin activity assay

Femurs were flushed with 300 μl of flushing buffer (10 mM EDTA in PBS). Bone marrow fluid was mixed 1:1 with the flushing buffer or, as a specificity control, buffer containing 10 U/ml hirudin (Sigma, H0393), and incubated for 5 minutes at 37 °C. Chromogenic thrombin substrate (1 mM, BIOPHEN CS 0138, ANIARA) was added and incubated for 10 minutes, followed by the addition of 2% citric acid to stop the reaction. Absorbance was determined at 405 nm against a blank. Thrombin activity was determined by subtracting non-specific substrate hydrolysis, (substrate turnover in the presence of hirudin) from substrate hydrolysis without hirudin, and activity was normalized to total protein in the femur, as determined by the Bradford assay.

Immunohistochemistry

Femurs, either fresh or fixed overnight at 4°C in 4% paraformaldehyde and exchanged with 30% sucrose for 2 days, were embedded in Optimal Cutting Temperature (OCT) compound (Sakura Finetek USA, Inc., Tissue-Tek) and 'snap-frozen' in *N*-methylbutane chilled in liquid nitrogen. Sections of 6- or 10-μm thickness were generated with a cryostat (Leika) at −24 °C with a tungsten carbide blade (Leica) and a CryoJane tape transfer system (Instrumedics). Sections were mounted on adhesive-coated slides (Leica), fixed in acetone and air-dried. Sections were stained by incubation either for 2 hours at room temperature or overnight at 4 °C with primary antibodies, followed by washing with PBS and 1 hour incubation of secondary antibody if needed and Hoechst for 5 minutes at room temperature, and were analyzed with an Olympus BX51 microscope and an Olympus DP71 camera or a Zeiss 710 confocal microscope with x 10, x 20 air objectives and x 40, x 60 and x 100 oil objectives for high resolution. EPCR was stained using either biotinylated anti-EPCR (1:100, clone 1560, eBioscience) followed by streptavidin 488 (Invitrogen) or conjugated EPCR-PE (1:50, clone 1560, eBioscience). TM was stained using rat anti mouse TM (1:200, clone 461714, R&D) followed by anti-rat 488 (Jackson ImmunoResearch) or TM-FITC conjugated antibody (1:100, clone 461714, R&D). PAR1 was detected using rabbit anti-mouse PAR1 (1:100, cline H-111, Santa Cruz) followed by staining with PE or FITC anti-rabbit antibody (Jackson ImmunoResearch). For CFU-F cultures, total bone marrow cells were cultured in 24 well plates on cover slips for 2–7 days. Before stimulation, samples were washed and treated with thrombin (1 U/ml) for 1 hour and fixed with 4% PFA. Following fixation and blocking with 7% horse serum, cover slips were subjected to immunostaining. For immunofluorescence studies in CFU-F culture, functional CXCL12 was detected using mouse anti CXCL12 antibody (1:50, clone K15C, either provided by F. Arenzana-Seisdedos Institute Pasteur, France or purchased from Millipore) followed by staining with PE anti-mouse antibody (Jackson ImmunoResearch). Functional CXCL12 was detected on PFA-fixed paraffin-embedded mouse bone sections with the use of the avidin-biotin-peroxidase complex method and DAB chromogen kit (Dako, Glostrup, Denmark) and the anti–CXCL12 monoclonal antibody K15C (1:50 dilution).

Imaging flow cytometry (*ImageStream*) analysis

Bone marrow MNCs were analyzed by Imaging Flow Cytometry using the *ImageStreamX* mark II instrument (Amnis-EMD Millipore, Seattle, WA) with IDEAS 6.0 software

(Amnis). Single-stained control cells were used to compensate fluorescence between channel images to avoid emission spectra overlap. Cells were gated for single cells with the area and aspect ratio features, and for focused cells with the Gradient RMS feature. Cells were then gated for the selection of positively stained cells using their pixel intensity, as set by the cutoff with IgG and secondary antibody control staining. For protein polarity calculations, we used the Delta Centroid XY feature, calculating the distance in microns between the intensity-weighted center of the fluorescence image and the geometric center of the bright field image for each image pair. This feature distinguishes between images with globally distributed staining (non-polar, lower Delta Centroid values) from those with capped staining (polar, higher Delta Centroid values). Intensity was calculated as the sum of the background subtracted pixel values. For Cdc42 staining, bone marrow-enriched MNC were first cultured on fibronectin (FN)/CXCL12 coated plates for 2 hours. Next, we collected both the adherent and non-adherent fractions (to collect both the $EPCR^+$ and $EPCR^-$ fractions) and stained for extracellular markers followed by intracellular Cdc42 staining.

Long-term competitive repopulation assays

HSC functional activity was assessed using competitive repopulation assays with the congenic Ly5.1/Ly5.2 system. Blood (500 μl) was obtained from B6.SJL (CD45.1) mice, collected from either PBS or thrombin treated mice, and then mixed with 2 x 10^5 total bone marrow cells from C57BL/6 (CD45.2) mice as competitors. Recipient C57BL/6 (CD45.2) mice were subjected to lethal irradiation (10 Gy) 5–16 hours before transplantation. For reconstitution after L-NAME and aPC treatment, bone marrow cells (2 x 10^5 or 1 x 10^5) from B6.SJL (CD45.1) mice, collected from mice treated either with PBS or L-NAME (30 mg/kg for 5 days), were mixed with 4 x 10^5 total bone marrow cells from C57BL/6 (CD45.2) mice as competitors. Recipient C57BL/6 (CD45.2) mice were subjected to lethal irradiation (10 Gy) 16 hours before transplantation. For bone marrow reconstitution after EPCR neutralization treatment, total bone marrow cells were treated *in vitro* with non-neutralizing (clone 1562) or neutralizing (clone 1560) anti-EPCR for 60 minutes at 37 °C. Following incubation, cells were washed and 2 x 10^5 donor cells were transplanted together with 4 x 10^5 recipient type bone marrow cells into lethally irradiated mice. For $Procr^{low}$ competitive repopulation assays, total bone marrow cells (2 x 10^5) from C57BL/6 or $Procr^{low}$ (CD45.2) mice were mixed with 4 x 10^5 total bone marrow cells from B6.SJL (CD45.1) recipient mice as competitors. Recipient B6.SJL (CD45.1) mice were subjected to lethal irradiation (10 Gy) 5–16 hours before transplantation. 16 weeks after transplantation, bone marrow cells were stained for CD45.1-PE (clone A20, eBioscience) and CD45.2-FITC (clone 104, Biolegend) and analyzed by flow cytometry.

Immunoblot analysis

Total protein (20 μg) of bone marrow supernatant following PBS or thrombin injection was TCA (trichloroacetic acid) precipitated, separated by 12% SDS-PAGE and transferred to nitrocellulose membranes. The membranes were blocked with Tris-buffered saline containing Tween-20 and 3% (weight/vol) BSA, and then probed with biotinylated-EPCR antibody clone 1560. As a positive control, we used the supernatant of mouse bEND.3

endothelial cells (obteined from Dr. Ronen Alon, Weizmann Institute, Israel) incubated with thrombin (1 U/ml) for 30 minutes.

Statistical analyses

All statistical analyses were conducted with Prism 4.0c version or Excel (*P<0.05, **P<0.01, ***P<0.001, "ns" represents non significance). All data are expressed as mean ± standard error (s.e.m) and all *n* numbers represent biological repeats. Unless indicated otherwise in figure legends, a Student's two-tailed unpaired t-test was used to determine the significance of the difference between means of two groups. One-way ANOVA or two-way ANOVA was used to compare means among three or more independent groups. Bonferroni or Tukey post-hoc tests were used to compare all pairs of treatment groups when the overall *P* value was <0.05. A normal distribution of the data was tested using the Kolmogorov–Smirnov test if the sample size allowed. If normal-distribution or equal-variance assumptions were not valid, statistical significance was evaluated using the Mann–Whitney test and the Wilcoxon signed rank test. Animals were randomly assigned to treatment groups. Tested samples were assayed in a blinded fashion.

Supplementary Material

Refer to Web version on PubMed Central for supplementary material.

Acknowledgments

Transgenic *Procr*^{low} mice were kindly provided by FJ Castellino (University of Notre Dame, Notre Dame, IN). *F2r*$^{-/-}$ and *F2rl2*$^{-/-}$ were kindly provided by P. Andrade-Gordon (Johnson & Johnson, Spring House, PA). *Thbd*$^{Pro/Pro}$ mice were kindly provided by H. Weiler (Blood Center of Wisconsin, WI). TACE prodomain was stained with rabbit anti-mouse TACE prodomain antibody, kindly provided by C. Blobel, (Hospital of Special Surgery NY, NY). We thank CE. Dunbar (NIH, Bethesda, MD) for critically reviewing this manuscript. We thank R. Rotkopf (Weizmann Institute of Science, IL) for his assistance in data statistical analysis. This study was partially supported by the Israel Science Foundation (851/13) grant, the Ernest and Bonnie Beutler Research Program of Excellence in Genomic Medicine and FP7-HEALTH-2010 (CELL-PID #261387) (T.L.) and NIH grants HL-31950 and HL-60742, BMBF 01EO1003, and the Humboldt Foundation (W.R.).

REFERENCES

1. Papayannopoulou T, Scadden DT. Stem-cell ecology and stem cells in motion. Blood. 2008; 111:3923–3930. [PubMed: 18398055]
2. Spiegel A, Kalinkovich A, Shivtiel S, Kollet O, Lapidot T. Stem cell regulation via dynamic interactions of the nervous and immune systems with the microenvironment. Cell Stem Cell. 2008; 3:484–492. [PubMed: 18983964]
3. Sugiyama T, Kohara H, Noda M, Nagasawa T. Maintenance of the hematopoietic stem cell pool by CXCL12-CXCR4 chemokine signaling in bone marrow stromal cell niches. Immunity. 2006; 25:977–988. [PubMed: 17174120]
4. Mendez-Ferrer S, et al. Mesenchymal and haematopoietic stem cells form a unique bone marrow niche. Nature. 2010; 466:829–834. [PubMed: 20703299]
5. Schajnovitz A, et al. CXCL12 secretion by bone marrow stromal cells is dependent on cell contact and mediated by connexin-43 and connexin-45 gap junctions. Nat Immunol. 2011; 12:391–398. [PubMed: 21441933]
6. Petit I, et al. G-CSF induces stem cell mobilization by decreasing bone marrow SDF-1 and up-regulating CXCR4. Nat Immunol. 2002; 3:687–694. [PubMed: 12068293]

7. Priestley GV, Ulyanova T, Papayannopoulou T. Sustained alterations in biodistribution of stem/progenitor cells in Tie2Cre+ alpha4(f/f) mice are hematopoietic cell autonomous. Blood. 2007; 109:109–111. [PubMed: 16931623]
8. Zhang Y, et al. Identification of CXCR4 as a new nitric oxide-regulated gene in human CD34+ cells. Stem Cells. 2007; 25:211–219. [PubMed: 17023512]
9. Karp JM, et al. Thrombin mediated migration of osteogenic cells. Bone. 2005; 37:337–348. [PubMed: 15964256]
10. Colognato R, et al. Differential expression and regulation of protease-activated receptors in human peripheral monocytes and monocyte-derived antigen-presenting cells. Blood. 2003; 102:2645–2652. [PubMed: 12805069]
11. Ramalho-Santos M, Yoon S, Matsuzaki Y, Mulligan RC, Melton DA. "Stemness": transcriptional profiling of embryonic and adult stem cells. Science. 2002; 298:597–600. [PubMed: 12228720]
12. Ho IA, et al. Matrix metalloproteinase 1 is necessary for the migration of human bone marrow-derived mesenchymal stem cells toward human glioma. Stem Cells. 2009; 27:1366–1375. [PubMed: 19489099]
13. Riewald M, Ruf W. Protease-activated receptor-1 signaling by activated protein C in cytokine-perturbed endothelial cells is distinct from thrombin signaling. J Biol Chem. 2005; 280:19808–19814. [PubMed: 15769747]
14. Aronovich A, et al. A novel role for factor VIII and thrombin/PAR1 in regulating hematopoiesis and its interplay with the bone structure. Blood. 2013; 122:2562–2571. [PubMed: 23982175]
15. Heissig B, et al. Recruitment of stem and progenitor cells from the bone marrow niche requires MMP-9 mediated release of kit-ligand. Cell. 2002; 109:625–637. [PubMed: 12062105]
16. Tjwa M, et al. Membrane-anchored uPAR regulates the proliferation, marrow pool size, engraftment, and mobilization of mouse hematopoietic stem/progenitor cells. J Clin Invest. 2009; 119:1008–1018. [PubMed: 19273908]
17. Tudpor K, et al. Thrombin receptor deficiency leads to a high bone mass phenotype by decreasing the RANKL/OPG ratio. Bone. 2015; 72:14–22. [PubMed: 25460576]
18. Balazs AB, Fabian AJ, Esmon CT, Mulligan RC. Endothelial protein C receptor (CD201) explicitly identifies hematopoietic stem cells in murine bone marrow. Blood. 2006; 107:2317–2321. [PubMed: 16304059]
19. Kent DG, et al. Prospective isolation and molecular characterization of hematopoietic stem cells with durable self-renewal potential. Blood. 2009; 113:6342–6350. [PubMed: 19377048]
20. Iwasaki H, Arai F, Kubota Y, Dahl M, Suda T. Endothelial protein C receptor-expressing hematopoietic stem cells reside in the perisinusoidal niche in fetal liver. Blood. 2010; 116:544–553. [PubMed: 20442369]
21. Wilson NK, et al. Combined Single-Cell Functional and Gene Expression Analysis Resolves Heterogeneity within Stem Cell Populations. Cell Stem Cell. 2015; 20:00162–00169.
22. Riewald M, Petrovan RJ, Donner A, Mueller BM, Ruf W. Activation of endothelial cell protease activated receptor 1 by the protein C pathway. Science. 2002; 296:1880–1882. [PubMed: 12052963]
23. Griffin JH, Zlokovic BV, Mosnier LO. Activated protein C: biased for translation. Blood. 2015; 125:2898–2907. [PubMed: 25824691]
24. Geiger H, et al. Pharmacological targeting of the thrombomodulin-activated protein C pathway mitigates radiation toxicity. Nat Med. 2012; 18:1123–1129. [PubMed: 22729286]
25. Hein L, Ishii K, Coughlin SR, Kobilka BK. Intracellular targeting trafficking of thrombin receptors. A novel mechanism for resensitization of a G protein-coupled receptor. J Biol Chem. 1994; 269:27719–27726. [PubMed: 7961693]
26. Steidl U, et al. Gene expression profiling identifies significant differences between the molecular phenotypes of bone marrow-derived and circulating human CD34+ hematopoietic stem cells. Blood. 2002; 99:2037–2044. [PubMed: 11877277]
27. Wautier F, Wislet-Gendebien S, Chanas G, Rogister B, Leprince P. Regulation of nestin expression by thrombin and cell density in cultures of bone mesenchymal stem cells and radial glial cells. BMC Neurosci. 2007; 8:104. [PubMed: 18053121]

28. Dar A, et al. Rapid mobilization of hematopoietic progenitors by AMD3100 and catecholamines is mediated by CXCR4-dependent SDF-1 release from bone marrow stromal cells. Leukemia. 2011; 25:1286–1296. [PubMed: 21494253]
29. Broxmeyer HE, et al. Rapid mobilization of murine and human hematopoietic stem and progenitor cells with AMD3100, a CXCR4 antagonist. J Exp Med. 2005; 201:1307–1318. [PubMed: 15837815]
30. Mendez-Ferrer S, Lucas D, Battista M, Frenette PS. Haematopoietic stem cell release is regulated by circadian oscillations. Nature. 2008; 452:442–U444. [PubMed: 18256599]
31. Gu JM, Katsuura Y, Ferrell GL, Grammas P, Esmon CT. Endotoxin and thrombin elevate rodent endothelial cell protein C receptor mRNA levels and increase receptor shedding in vivo. Blood. 2000; 95:1687–1693. [PubMed: 10688825]
32. Qu D, Wang Y, Esmon NL, Esmon CT. Regulated endothelial protein C receptor shedding is mediated by tumor necrosis factor-alpha converting enzyme/ADAM17. J Thromb Haemost. 2007; 5:395–402. [PubMed: 17155946]
33. Wong, E.; Sagi, I. The 7th Congress of the Federation of the Israel Societies for Experimental Biology. Vol. PB-460. Israel: Eilat; 2014. ADAM17: master regulator in different IBD mice models, a study with evolutionary designed inhibitor pro-domain.
34. Stearns-Kurosawa DJ, Kurosawa S, Mollica JS, Ferrell GL, Esmon CT. The endothelial cell protein C receptor augments protein C activation by the thrombin-thrombomodulin complex. Proc Natl Acad Sci U S A. 1996; 93:10212–10216. [PubMed: 8816778]
35. Disse J, et al. The endothelial protein C receptor supports tissue factor ternary coagulation initiation complex signaling through protease-activated receptors. J Biol Chem. 2011; 286:5756–5767. [PubMed: 21149441]
36. Gu JM, et al. Disruption of the endothelial cell protein C receptor gene in mice causes placental thrombosis and early embryonic lethality. J Biol Chem. 2002; 277:43335–43343. [PubMed: 12218060]
37. Castellino FJ, et al. Mice with a severe deficiency of the endothelial protein C receptor gene develop, survive, and reproduce normally, and do not present with enhanced arterial thrombosis after challenge. Thromb Haemost. 2002; 88:462–472. [PubMed: 12353077]
38. Weiler-Guettler H, et al. A targeted point mutation in thrombomodulin generates viable mice with a prethrombotic state. J Clin Invest. 1998; 101:1983–1991. [PubMed: 9576763]
39. Wang L, Yang L, Filippi MD, Williams DA, Zheng Y. Genetic deletion of Cdc42GAP reveals a role of Cdc42 in erythropoiesis and hematopoietic stem/progenitor cell survival, adhesion, and engraftment. Blood. 2006; 107:98–105. [PubMed: 16174757]
40. Geiger H, Koehler A, Gunzer M. Stem cells, aging, niche, adhesion and Cdc42: a model for changes in cell-cell interactions and hematopoietic stem cell aging. Cell Cycle. 2007; 6:884–887. [PubMed: 17404508]
41. Florian MC, et al. Cdc42 activity regulates hematopoietic stem cell aging and rejuvenation. Cell Stem Cell. 2012; 10:520–530. [PubMed: 22560076]
42. Papayannopoulou T, Priestley GV, Nakamoto B. Anti-VLA4/VCAM-1-induced mobilization requires cooperative signaling through the kit/mkit ligand pathway. Blood. 1998; 91:2231–2239. [PubMed: 9516120]
43. Taniguchi Ishikawa E, et al. Klf5 controls bone marrow homing of stem cells and progenitors through Rab5-mediated beta1/beta2-integrin trafficking. Nat Commun. 2013; 4:1660. [PubMed: 23552075]
44. Williams DA, Zheng Y, Cancelas JA. Rho GTPases and regulation of hematopoietic stem cell localization. Methods Enzymol. 2008; 439:365–393. [PubMed: 18374178]
45. North TE, et al. Hematopoietic stem cell development is dependent on blood flow. Cell. 2009; 137:736–748. [PubMed: 19450519]
46. Adamo L, et al. Biomechanical forces promote embryonic haematopoiesis. Nature. 2009; 459:1131–1135. [PubMed: 19440194]
47. Aicher A, et al. Essential role of endothelial nitric oxide synthase for mobilization of stem and progenitor cells. Nat Med. 2003; 9:1370–1376. [PubMed: 14556003]

48. Kolluru GK, Siamwala JH, Chatterjee S. eNOS phosphorylation in health and disease. Biochimie. 2010; 92:1186–1198. [PubMed: 20363286]
49. Wang D, et al. Identification of multipotent mammary stem cells by protein C receptor expression. Nature. 2015; 517:81–84. [PubMed: 25327250]
50. Schaffner F, et al. Endothelial protein C receptor function in murine and human breast cancer development. PLoS One. 2013; 8:e61071. [PubMed: 23593394]
51. Pepler L, Yu P, Dwivedi DJ, Trigatti BL, Liaw PC. Characterization of mice harboring a variant of EPCR with impaired ability to bind protein C: Novel role of EPCR in hematopoiesis. Blood. 2015
52. Sanjuan-Pla A, et al. Platelet-biased stem cells reside at the apex of the haematopoietic stem-cell hierarchy. Nature. 2013; 502:232–236. [PubMed: 23934107]
53. Zhao M, et al. Megakaryocytes maintain homeostatic quiescence and promote post-injury regeneration of hematopoietic stem cells. Nat Med. 2014; 20:1321–1326. [PubMed: 25326798]
54. Bruns I, et al. Megakaryocytes regulate hematopoietic stem cell quiescence through CXCL4 secretion. Nat Med. 2014; 20:1315–1320. [PubMed: 25326802]
55. Slungaard A, et al. Platelet factor 4 enhances generation of activated protein C in vitro and in vivo. Blood. 2003; 102:146–151. [PubMed: 12609838]
56. Ludin A, et al. Monocytes-macrophages that express alpha-smooth muscle actin preserve primitive hematopoietic cells in the bone marrow. Nat Immunol. 2012; 13:1072–1082. [PubMed: 22983360]
57. Yang L, et al. Rho GTPase Cdc42 coordinates hematopoietic stem cell quiescence and niche interaction in the bone marrow. Proc Natl Acad Sci U S A. 2007; 104:5091–5096. [PubMed: 17360364]
58. Yang FC, et al. Rac and Cdc42 GTPases control hematopoietic stem cell shape, adhesion, migration, and mobilization. Proc Natl Acad Sci U S A. 2001; 98:5614–5618. [PubMed: 11320224]
59. Esmon CT. Crosstalk between inflammation and thrombosis. Maturitas. 2004; 47:305–314. [PubMed: 15063484]
60. Wang L, et al. A blood flow-dependent klf2a–NO signaling cascade is required for stabilization of hematopoietic stem cell programming in zebrafish embryos. Blood. 2011; 118:4102–4110. [PubMed: 21849483]
61. Damiano BP, et al. Cardiovascular responses mediated by protease-activated receptor-2 (PAR-2) and thrombin receptor (PAR-1) are distinguished in mice deficient in PAR-2 or PAR-1. J Pharmacol Exp Ther. 1999; 288:671–678. [PubMed: 9918574]
62. Darrow AL, et al. Biological consequences of thrombin receptor deficiency in mice. Thromb Haemost. 1996; 76:860–866. [PubMed: 8972001]
63. Xu J, Ji Y, Zhang X, Drake M, Esmon CT. Endogenous activated protein C signaling is critical to protection of mice from lipopolysaccaride-induced septic shock. J Thromb Haemost. 2009; 7:851–856. [PubMed: 19320827]
64. Dickinson CD, Ruf W. Active site modification of factor VIIa affects interactions of the protease domain with tissue factor. J Biol Chem. 1997; 272:19875–19879. [PubMed: 9242651]

The coagulation factors thrombin, PAR1, aPC and EPCR, unexpectedly and independently also control the nitric oxide production switch in hematopoietic stem cells, thereby regulate EPCR-expressing stem cell adhesion and retention in the bone marrow versus their recruitment to the blood.

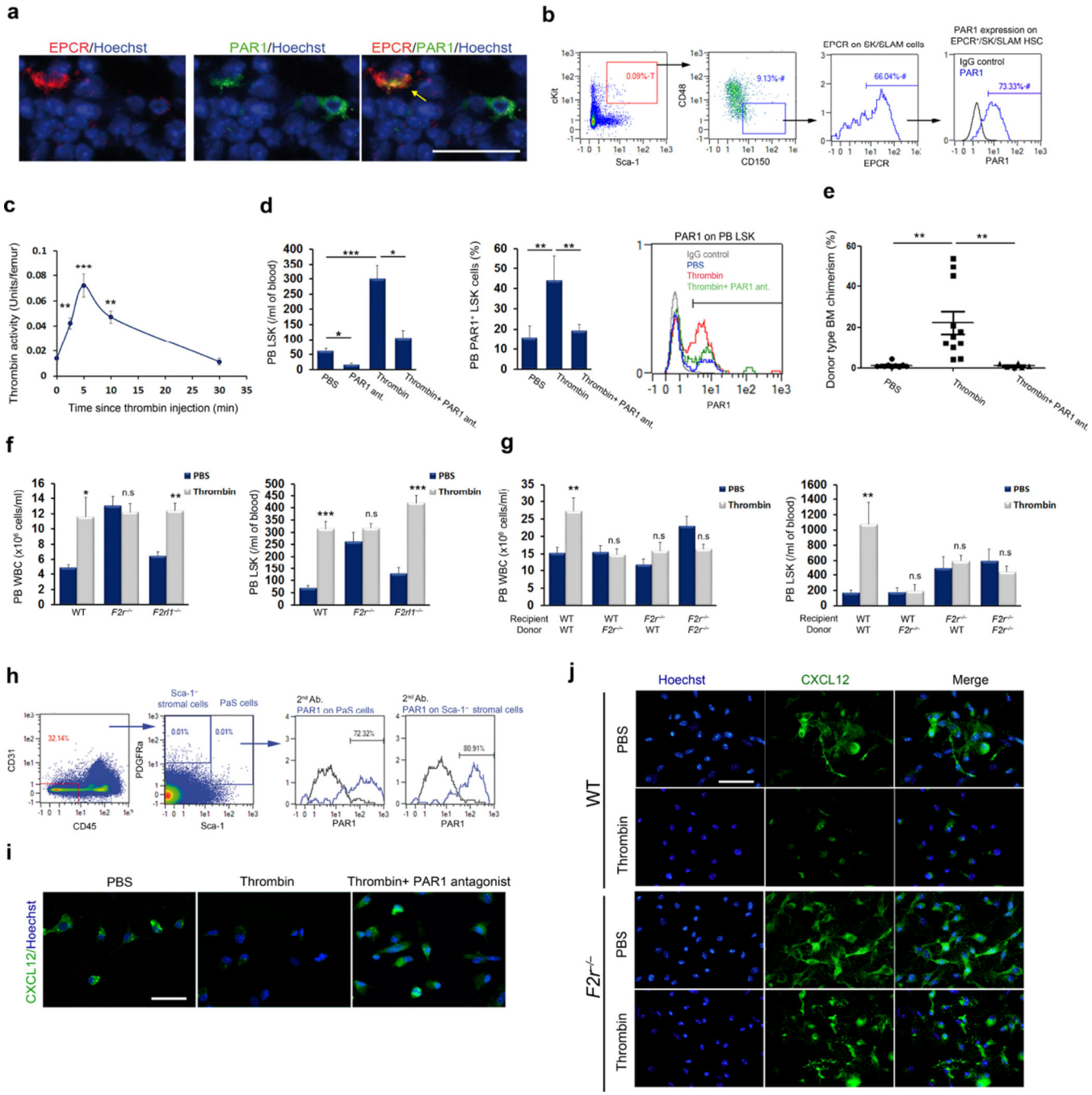

Figure 1. Thrombin-PAR1 signaling induces HSC recruitment

(a) Immunohistochemistry for EPCR (red), PAR1 (green) and nuclei (blue) in bone marrow of wild-type mice; scale bar, 20 μm. (**b**) FACS analysis of PAR1 expression by bone marrow EPCR$^+$ SK/SLAM cells. The letter 'T' represents percentage out of total population and the '#' symbol represents percentage out of the previous gate. (**c**) Thrombin activity in the bone marrow measured at the indicated times following thrombin injection; $n = 5$. (**d**) Peripheral blood (PB) LSK and PAR1$^+$ LSK cells ($n = 4$) following thrombin injection with ($n = 8$) or without ($n = 14$) PAR1 antagonist; P values, one-way ANOVA with Tukey's

post-test. (**e**) Long-term competitive reconstitution assays of thrombin-mobilized HSCs, with or without PAR1 antagonist, versus PBS control. Donor cell chimerism 16 weeks after transplantation is plotted; each dot represents one mouse. *P* values, one-way ANOVA with Tukey's post-test. (**f**) Circulating white blood cells (WBC) and LSK cells in wild-type (WT), *F2r*$^{-/-}$ or *F2rl1*$^{-/-}$ mice following thrombin injection; $n = 4$, *P* values, two-way ANOVA with Tukey's post-test. (**g**) Circulating WBC and LSK cells following thrombin treatment of wild-type ($n = 8$) or *F2r*$^{-/-}$ bone marrow chimeras; $n = 8$ for hematopoietic *F2r*$^{-/-}$ chimeras and $n = 4$ for stromal *F2r*$^{-/-}$ chimeras. *P* values, two-way ANOVA with Bonferroni post-test. (**h**) FACS analysis of PAR1 expression by PDGFRα^{+}Sca1^{+}CD45^{-}CD31^{-} PαS cells and Sca-1^{-} stromal cells isolated from the bone marrow of wild-type mice. (**i**) Immunohistochemistry staining of CXCL12 (green) and nuclei (blue) in stromal cultures of wild-type bone marrow, stimulated with thrombin with or without PAR1 antagonist; scale bar, 20 μm. (**j**) Immunohistochemistry staining of CXCL12 (green) and nuclei (blue) in stromal cultures of wild-type or *F2r*$^{-/-}$ bone marrow with or without thrombin stimulation; scale bar, 20 μm.

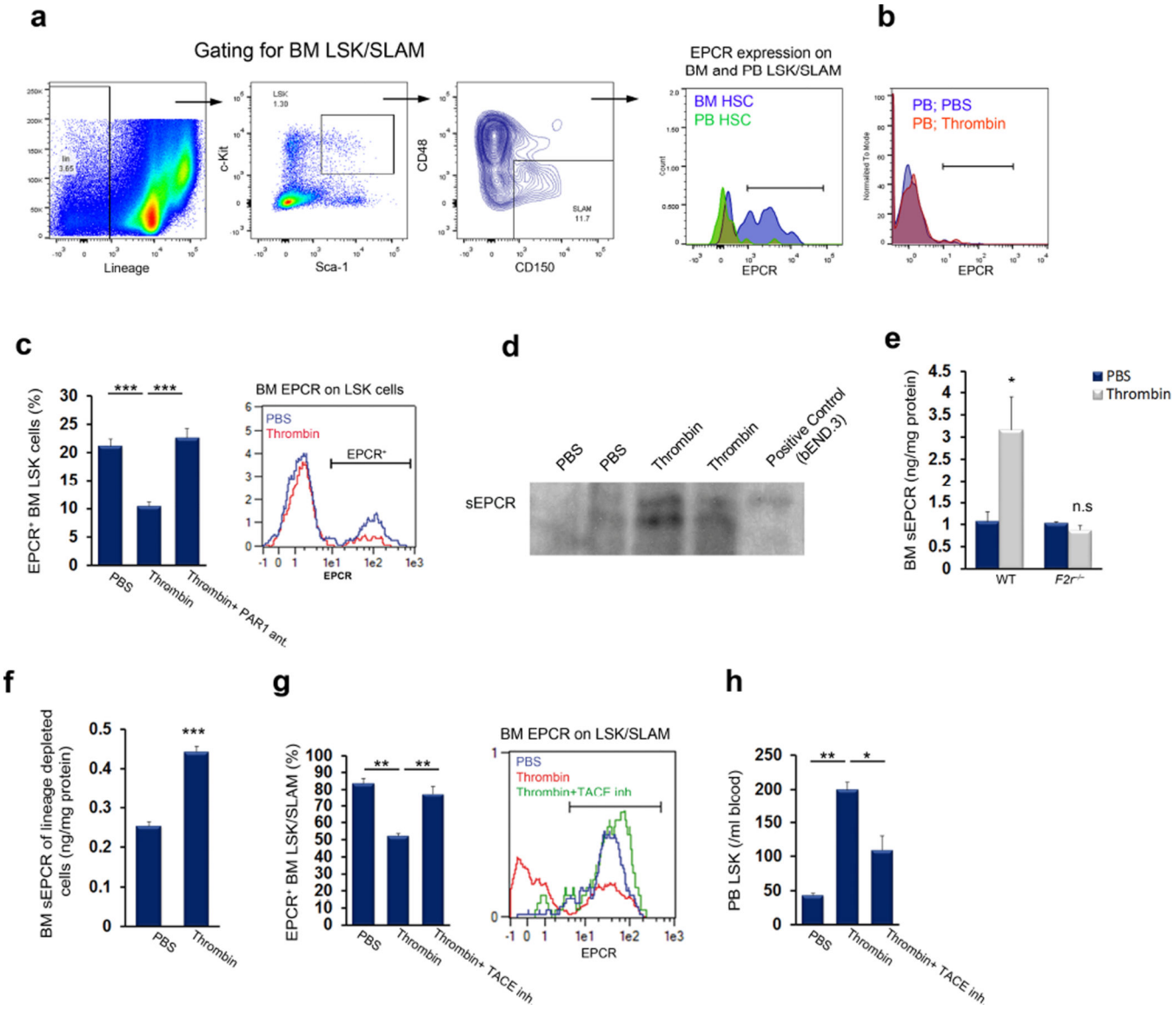

Figure 2. Thrombin-PAR1-dependent EPCR shedding induces HSC mobilization

(**a**) FACS analysis of EPCR expression on circulating and bone marrow (BM) LSK SLAM cells; representative data are shown for 4 mice. (**b**) FACS analysis of EPCR expression on circulating LSK cells in mice treated with thrombin or PBS; representative data are shown for 4 mice. (**c**) Bone marrow EPCR^{+} LSK cells following thrombin injection with (n = 4) or without (n = 8) administration of a PAR1 antagonist; P values, one-way ANOVA with Tukey's post-test. (**d,e**) Soluble EPCR (sEPCR) in bone marrow fluid 1 hour after thrombin injection, as measured by western blotting (**d**) or ELISA (**e**) in wild-type or $F2r^{-/-}$ mice; n = 4. (**f**) sEPCR ELISA following thrombin stimulation *in vitro* in lineage-depleted bone marrow cells; n = 4. (**g,h**) Bone marrow EPCR^{+} LSK SLAM cells (**g**) and peripheral blood LSK cells (**h**) in PBS or thrombin-treated mice, with or without pretreatment with TACE inhibitor for 1 hour before thrombin injection; n = 4; P values, one-way ANOVA with Tukey's post-test.

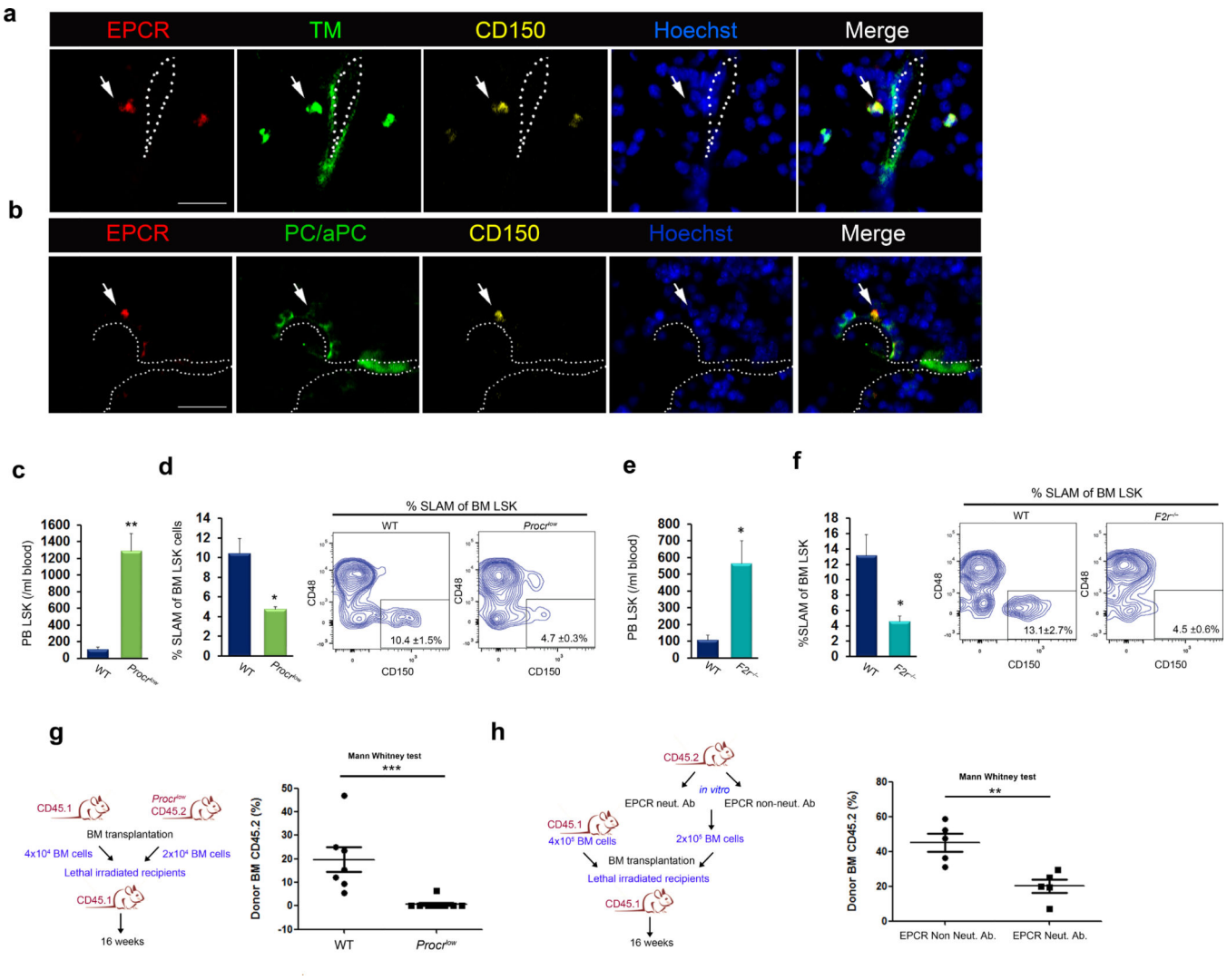

Figure 3. A TM- and aPC-enriched bone marrow endothelial microenvironment regulates EPCR$^+$ HSC retention

(**a**) Immunohistochemistry for EPCR (red), thrombomodulin (TM; green), CD150 (yellow) and nuclei (blue) in the bone marrow of wild-type mice. Scale bar, 20 μm. (**b**) Immunohistochemistry for EPCR (red), PC/aPC (green), CD150 (yellow) and nuclei (blue) in the bone marrow of wild-type mice. Scale bar, 20 μm. (**c**) Circulating LSK cells and (**d**) bone marrow LSK SLAM cells in wild-type or *Procr*^{low} mice; mean ± s.e.m, $n = 4$. (**e,f**) Circulating LSK cells (**e**) and bone marrow LSK SLAM cells (**f**) in wild-type or *F2r*$^{-/-}$ mice; $n = 4$. (**g**) Bone marrow competitive repopulation assay using bone marrow from wild-type and *Procr*^{low} mice. Repopulation was assessed 16 weeks following transplantation; each dot represents an individual recipient mouse. *P* values, one-way ANOVA with Mann-Whitney post-test. (**h**) Bone marrow competitive repopulation assay of wild-type bone marrow cells pretreated with either EPCR non-inhibitory or EPCR neutralizing antibody for 60 minutes. Repopulation was assessed 16 weeks following transplantation; each dot represents an individual recipient mouse. *P* values, one-way ANOVA with Mann-Whitney post-test.

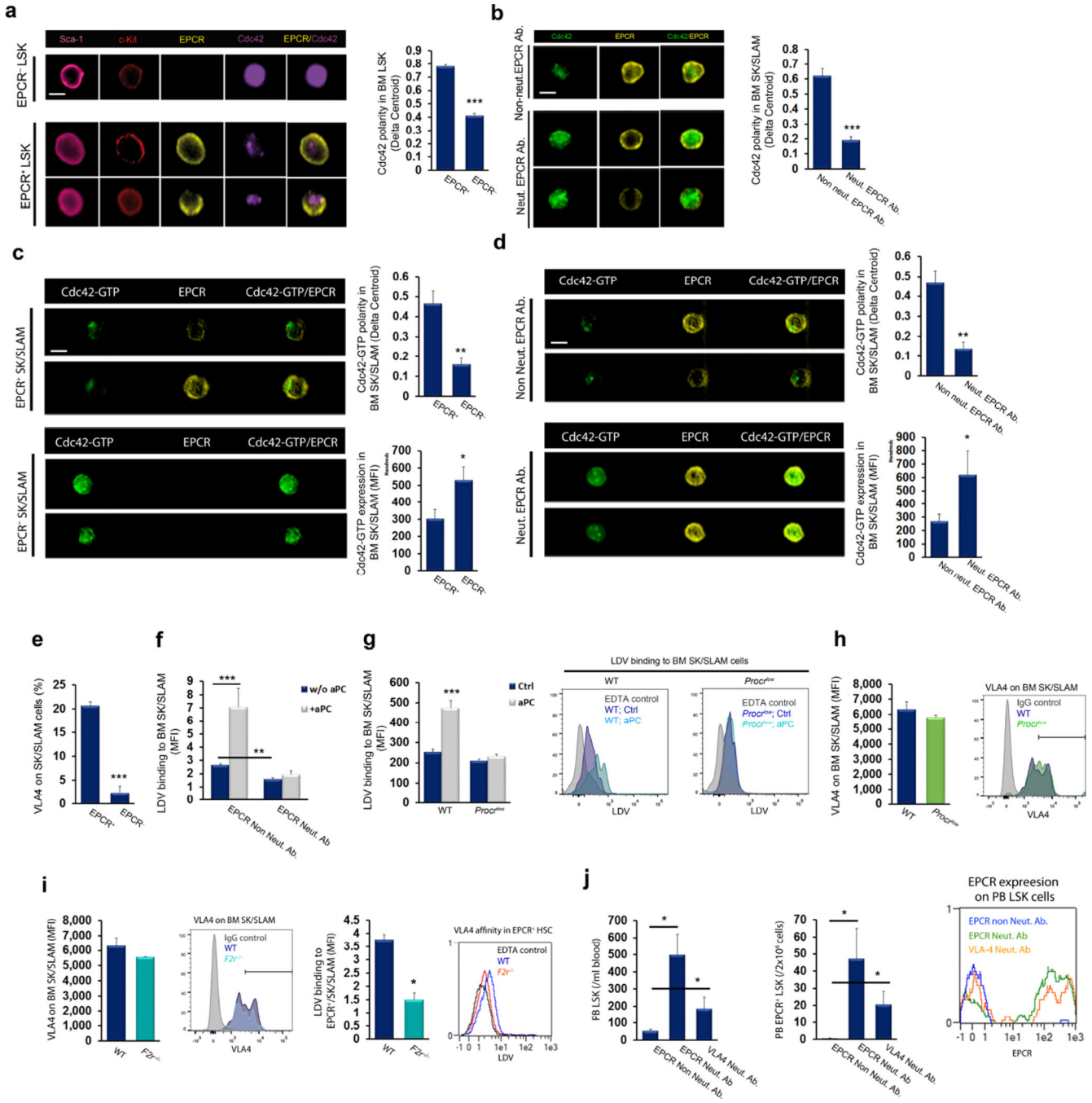

Figure 4. aPC-EPCR-PAR1 signaling retains HSCs by inducing Cdc42 polarity and stabilizing VLA4

(**a**) Cdc42 (purple) distribution in bone marrow EPCR$^+$ (yellow) and EPCR$^-$ Lineage negative Sca-1$^+$ (pink) c-Kit$^+$ (red) cells. Scale bar, 7 μm; $n = 4$. (**b**) Cdc42 (green) distribution in bone marrow EPCR$^+$ (yellow) SK SLAM cells pretreated with EPCR non-inhibitory or EPCR neutralizing antibody. Scale bar, 7 μm; $n = 5$. (**c**) Active Cdc42-GTP (green) in bone marrow EPCR$^+$ SK SLAM (yellow) and EPCR$^-$ LSK cells. Scale bar, 7 μm; $n = 5$. (**d**) Active Cdc42-GTP (green) in bone marrow EPCR$^+$ (yellow) SK SLAM cells

pretreated with EPCR non-inhibitory or EPCR neutralizing antibody. Scale bar, 7 μm; *n* = 4. (**e**) VLA4 expression on bone marrow $EPCR^+$ or $EPCR^-$ SK SLAM cells; *n* = 4. (**f**) VLA4 affinity measured by LDV probe binding to bone marrow $EPCR^+$ SK SLAM cells following *in vitro* stimulation with aPC of cells that had been pretreated with EPCR neutralizing antibody or control EPCR non-inhibitory antibody for 30 minutes; *n = 7*. (**g**) VLA4 affinity of bone marrow SK SLAM cells from wild-type or $Procr^{low}$ mice following *in vitro* treatment with aPC for 1 hour; *n* = 3. (**h**) VLA4 expression on bone marrow SK SLAM cells from wild-type or $Procr^{low}$ mice; *n* = 3. (**i**) VLA4 expression on bone marrow SK SLAM cells and VLA4 affinity on bone marrow $EPCR^+$ SK SLAM cells from wild-type or $F2r^{-/-}$ mice; *n* = 3. (**j**) Peripheral blood LSK and $EPCR^+$ LSK cell frequencies following EPCR or VLA4 neutralization *in vivo*; *n* = 4, *P* values, one-way ANOVA with Tukey's post-test for left panel and Dunn's post-test for right panel.

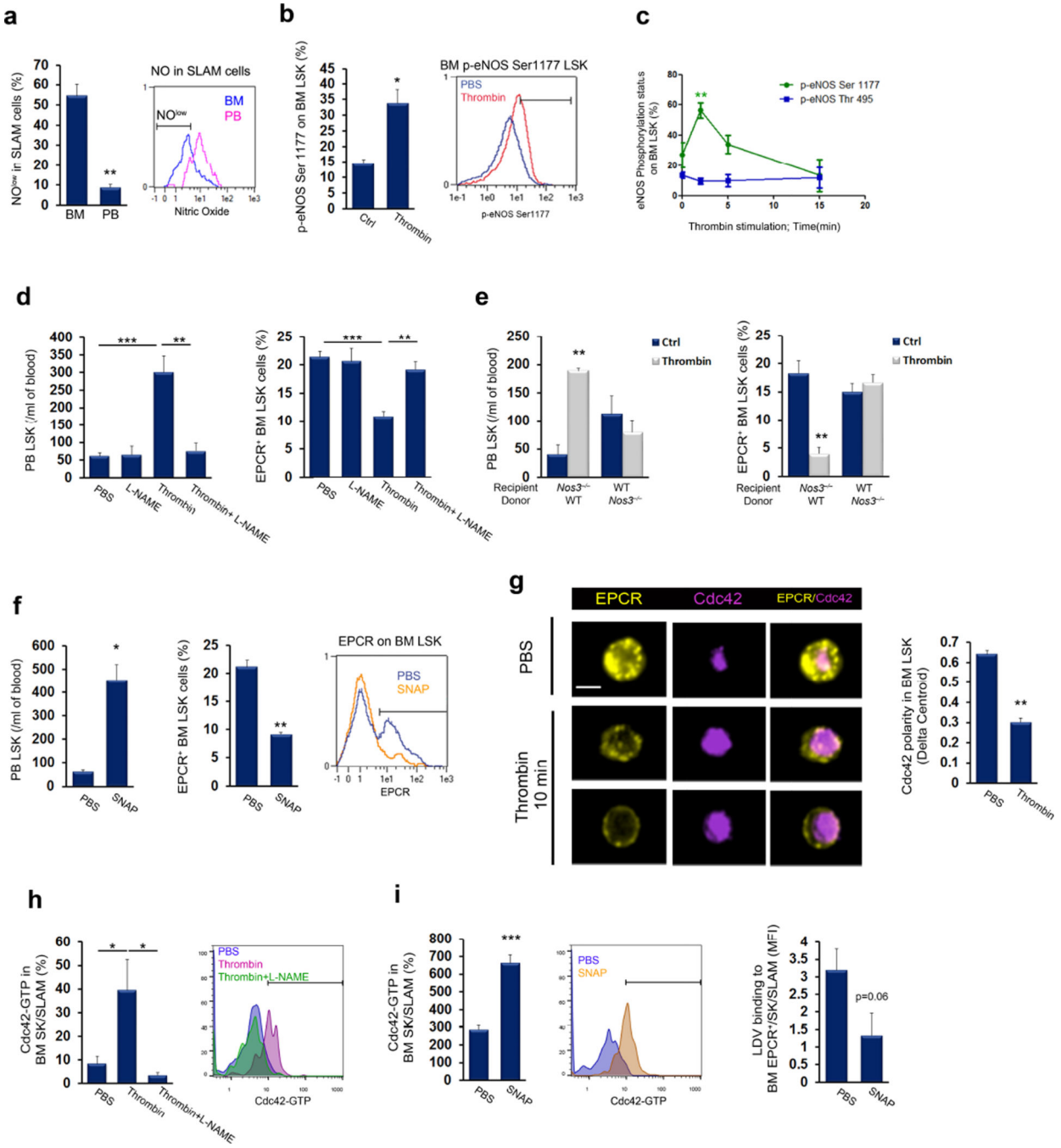

Figure 5. Thrombin-PAR1 signaling induces NO production and HSC mobilization

(**a**) NO levels in SLAM cells obtained from the bone marrow and peripheral blood. NO^{low} gating represents baseline reactivity; $n = 3$. (**b**) FACS analysis of eNOS Ser1177 phosphorylation in BM LSK cells 30 minutes following thrombin injection; $n = 4$. (**c**) Kinetics of eNOS phosphorylation on Ser1177 and Thr495 in bone marrow LSK cells following *in vitro* thrombin stimulation; $n = 4$. (**d**) Circulating LSK cells and bone marrow $EPCR^+$ LSK cells following thrombin injection in mice pretreated with or without L-NAME; $n = 6$, *P* values, one-way ANOVA with Tukey's post-test. (**e**) Circulating LSK cells and

bone marrow EPCR$^+$ LSK cells in wild-type or *Nos3*$^{-/-}$ bone marrow chimeric mice following thrombin injection; $n = 4$. (**f**) Circulating LSK cells and bone marrow EPCR$^+$ LSK cells 60 minutes after SNAP injection; $n = 4$. (**g**) Cdc42 (purple) distribution on bone marrow EPCR$^+$ (yellow) LSK cells 10 minutes following *in vivo* thrombin treatment. Scale bar, 7 μm. (**h**) FACS analysis of Cdc42-GTP following *in vitro* thrombin treatment for 15 minutes of bone marrow SK SLAM cells that had been pretreated with or without L-NAME for 2 hours; $n = 4$, *P* values, one-way ANOVA with Tukey's post-test. (**i**) Cdc42-GTP in bone marrow SK SLAM cells (left) and LDV-FITC binding to bone marrow EPCR$^+$ SK SLAM cells (right) following *in vitro* treatment with SNAP for 15 minutes; $n = 4$.

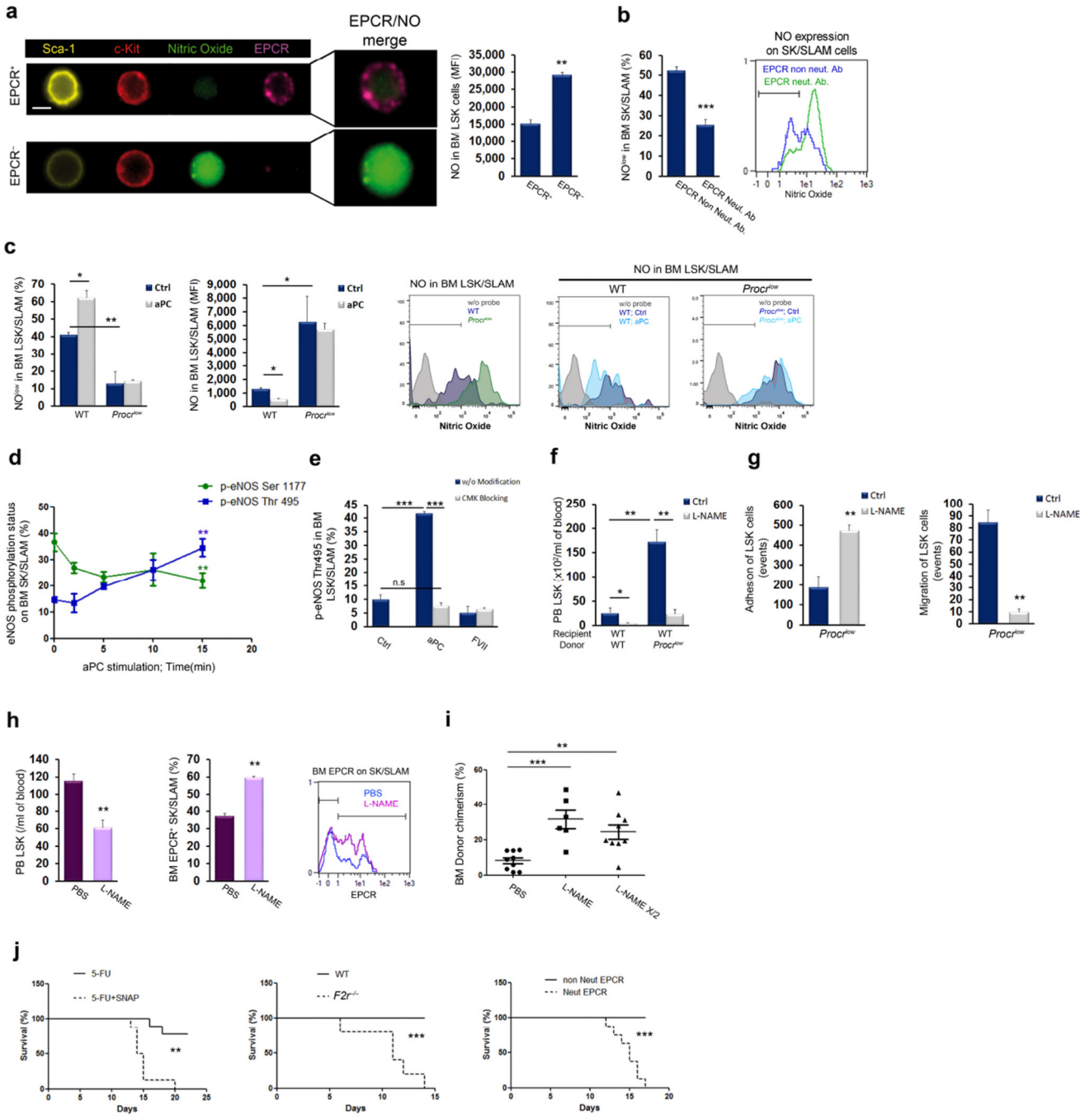

Figure 6. aPC-EPCR signaling limits NO production and promotes LT-HSC retention

(**a**) NO (green) levels in BM LSK EPCR^{+} (purple) and EPCR^{-} lineage negative Sca-1^{+} (yellow) c-Kit^{+} (red) cells. Scale bar, 7 μm. (**b**) Percentage of NO^{low} SK SLAM cells following *in vitro* treatment of bone marrow cells with EPCR neutralizing or non-neutralizing antibody; $n = 4$. (**c**) Percentage of NO^{low} cells and NO levels in wild-type or *Procr*^{low} bone marrow LSK SLAM cells, with or without *in vitro* aPC treatment for 1 hour; $n = 3$, P values, two-way ANOVA with Bonferroni post-test. (**d**) Kinetics of eNOS phosphorylation on Ser1177 or Thr495 in bone marrow SK SLAM cells following *in vitro*

aPC stimulation; $n = 4$. (**e**) eNOS phosphorylation on Thr495 in bone marrow LSK SLAM cells following *in vitro* stimulation with aPC for 15 minutes, active-site blocked aPC, FVIIa, or active-site blocked FVIIa; $n = 4$, *P* values, one-way ANOVA with Tukey's post-test. (**f**) Circulating LSK cells in wild-type or $Procr^{low}$ chimeric mice following prolonged L-NAME treatment for 5 days; $n = 5$, *P* values, two-way ANOVA with Bonferroni post-test. (**g**) Adhesion and migration of $Procr^{low}$ bone marrow LSK cells following *in vitro* L-NAME or PBS treatment for 2 hours; $n = 6$. (**h**) Circulating LSK ($n = 8$), bone marrow $EPCR^{+}$ SK SLAM cells ($n = 4$) and representative FACS plot for EPCR expression following prolonged L-NAME or PBS treatment for 5 days. (**i**) Competitive repopulation of bone marrow cells obtained from donors treated with L-NAME or PBS, assessed 16 weeks following transplantation; each dot represents an individual recipient mouse; *P* values, one-way ANOVA with Tukey's post-test. (**j**) Survival after 5-FU treatment, with or without SNAP treatment ($n = 9$, *** *P* value = 0.0003), in wild-type vs *F2r*−/− mice ($n = 5$, ** *P* value= 0.0010) or co-treated with EPCR neutralizing or non-inhibitory antibody ($n = 9$, *** *P* value < 0.0001).